Bioorganic & Medicinal Chemistry 17 (2009) 5933–5949

Contents lists available at ScienceDirect

Bioorganic & Medicinal Chemistry

journal homepage: www.elsevier.com/locate/bmc

α-Substituted norstatines as the transition-state mimic in inhibitors of multiple digestive vacuole malaria aspartic proteases

Kristina M. Orrling [a], Melissa R. Marzahn [b], Hugo Gutiérrez-de-Terán [c], Johan Åqvist [d], Ben M. Dunn [b], Mats Larhed [a,*]

[a] Department of Medicinal Chemistry, Division of Organic Pharmaceutical Chemistry, Uppsala University, BMC, Box 574, 75 123 Uppsala, Sweden
[b] Biochemistry and Molecular Biology, College of Medicine, University of Florida, PO Box 100245, Gainsville, FL, USA
[c] Fundación Pública Galega de Medicina Xenómica, Hospital Clínico de Santiago de Compostela, 15705 Santiago de Compostela, Spain
[d] Department of Cell and Molecular Biology, BMC, Uppsala University, Box 596, 751 23 Uppsala, Sweden

ARTICLE INFO

Article history:
Received 7 May 2009
Revised 24 June 2009
Accepted 28 June 2009
Available online 3 July 2009

Keywords:
Malaria
Plasmepsin
Inhibitors
Microwave-assisted synthesis
Molecular dynamics
Linear interaction energy mehtod

ABSTRACT

The impact of moving the P1 side-chain from the β-position to the α-position in norstatine-containing plasmepsin inhibitors was investigated, generating two new classes of tertiary alcohol-comprising α-benzylnorstatines *and* α-phenylnorstatines. Twelve α-substituted norstatines were designed, synthesized and evaluated for their inhibitory potencies against plasmepsin II and the plasmepsin IV orthologues (PM4) present in the digestive vacuole of all four *Plasmodium* species causing malaria in man. New synthetic routes were developed for producing the desired α-substituted norstatines as pure stereoisomers. The best compounds provided K_i values in the nanomolar range for all PM4, with a best value of 110 nM in PM4 from *Plasmodium ovale*. In addition, excellent selectivity over the closely related human aspartic protease Cathepsin D was achieved. The loss of affinity to *Plasmodium falciparum* PM4, which was experienced upon the move of the P1 substituent, was rationalized by the calculation of inhibitor–protein binding affinities using the linear interaction energy method (LIE).

1. Introduction

Malaria is a major cause of death, illness and poverty for approximately half of the world's population.[1] It is a parasite-inflicted disease, which is spread throughout the tropical regions of the world by female mosquitoes of the genus *Anopheles*. Four species of protozoal parasites of the *Plasmodium* genus cause malaria in humans, *Plasmodium falciparum* (Pf), *Plasmodium malariae* (Pm), *Plasmodium ovale* (Po) and *Plasmodium vivax* (Pv). Despite considerable scientific advances and the development of new drugs, malaria is reported to cause over one million fatal cases annually, the majority being children under the age of five.[1] The constant emergence of parasitic strains resistant to the currently available antimalarials implies an acute need for new therapeutic agents with novel routes of action.[2]

In 1990, Goldberg et al. found that pepstatin A, a modified peptide which inhibits most aspartic proteases, drastically reduced the rate of the hemoglobin degradation in the parasite digestive vacuole (DV).[3] In subsequent studies, 10 aspartic proteases (plasmepsins) were identified to be encoded in the genome of Pf, the most lethal malaria species.[4,5] Four of these, plasmepsin I (PfPM1), II (PfPM2) and IV (PfPM4) and the highly homologous histo-aspartic protease, HAP (aka PfPM3), are involved in the hemoglobin proteolysis in the DV.[6,7] Furthermore, the solution of the first X-ray inhibitor–enzyme cocrystal structure of PfPM2 in 1996 made structure-based drug discovery efforts possible. Despite substantial enzyme flexibility and difficult modeling, several groups have since then reported on novel PfPM2 inhibitors which were found to be active in nanomolar concentrations.[8–10] Most of the recently published inhibitors of the Pf DV plasmepsin have been peptidomimetic in structure, using different transition-state (TS) isosteres, with lipophilic side-chains. In the three other malaria parasites that infect humans, only the orthologues of PfPM4 have been isolated from the DV (PmPM4, PoPM4 and PvPM4).[11] This indicates that PM4 might be the most relevant DV plasmepsin to target. As the active site is highly conserved in these iso-enzymes, it has been hypothesized that an inhibitor of PfPM4 would reduce the parasitaemia regardless of the infecting species.[11–13] However, there is evidence for redundancy of DV plasmepsins in Pf, which indicates that all four Pf paralogues might have to be targeted to effectively abate the parasite.[14–16]

The structural starting point for this study was the compound **KNI-10006**, reported by Kiso in 2003 (Fig. 1).[17] This norstatine-based lead structure possesses nanomolar inhibition of all four plasmepsins in the DV of Pf, and is remarkably potent in the case of PfPM2 and PfPM4 with IC_{50} values of 39 nM and 15 nM, respectively. The K_i value for PfPM2 was determined to be in the

* Corresponding author. Fax: +46 18 471 4882.
E-mail address: Mats.Larhed@orgfarm.uu.se (M. Larhed).

0968-0896/$ - see front matter © 2009 Elsevier Ltd. All rights reserved.
doi:10.1016/j.bmc.2009.06.065

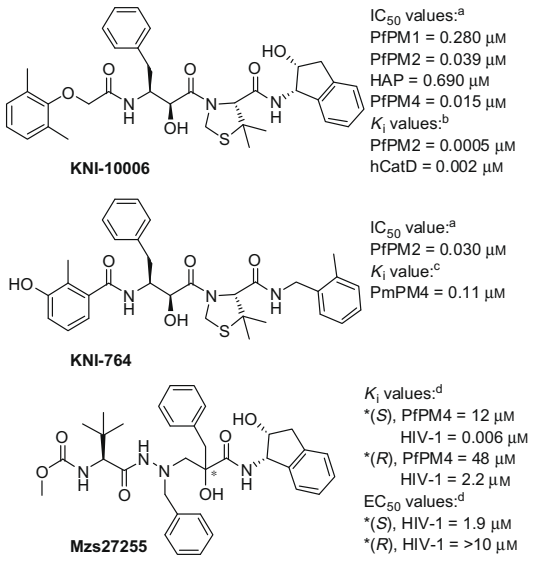

Figure 1. Phenylnorstatine and α-phenylnorstatine lead structures. (a) IC_{50} values for plasmepsins reported by Nezami et al.,[17] (b) K_i values reported by Kiso et al.,[18] (c) K_i value for PmPM4 reported by Clemente et al.,[13] (d) K_i values for HIV-1 refer to the inhibition of HIV-1 protease and the EC_{50} values refer to the efficacy on infected cells, according to Ekegren et al.[19] The PfPM4 data of **Mz27255** have not been published elsewhere.

0.5 ± 1 nM range. However, having a good activity towards several of aspartic proteases, **KNI-10006** was also found to be an efficacious inhibitor (K_i = 2 nM)[18] of the most closely related human aspartic protease, cathepsin D (hCatD). Another disadvantage with this compound was the low capacity to reduce parasite growth in Pf-infected erythrocyte cultures (IC_{50} = 6.8 μM), a shortcoming which partly might be explained by insufficient cell/vacuole membrane permeability.[18] A closely related compound, **KNI-764**, has been co-crystallized in PmPM4, showing an unexpected binding mode with the prime side of the compound binding to the non-prime sub-pockets in the active site of the enzyme.[13]

Previous experiences with a *tert*-hydroxy containing TS mimic for inhibition of another aspartic protease, HIV-1 protease, proved the possibility of retaining high potency, while improving membrane permeability in the Caco-2 cell assay.[19–21] One of the HIV-1 protease inhibitors comprising a tertiary alcohol, (*S*)-**Mzs27255**,[19] also showed some inhibitory activity on PfPM4 (K_i = 12 μM) (Fig. 1). These findings prompted us to evaluate the concept of utilizing masked tertiary alcohols for inhibition of plasmepsins by synthesizing novel inhibitors with an α-substituted norstatine core of type **A** (Fig. 2). In the phenylnorstatines (e.g., **KNI-10006** and **KNI-764**), the α-hydroxyl is tethered to the P1-phenyl by a two-carbon backbone linker, while in α-phenylnorstatines, the benzyl group is moved to the α-carbon adjacent to the carbonyl and the linker is reduced to only one carbon. Therefore, we decided to synthesize and evaluate inhibitors with an α-phenylnorstatine scaffold, as well as structures with an α-benzylnorstatine scaffold (Fig. 2). In order to further reduce the L-peptidic character of the inhibitors, the L-thioproline pseudoresidue in P1′, used in the **KNI** compounds, was complemented with compounds incorporating the analogue with D-configuration. In 2005, Beyer et al. showed that the DV plasmepsins accommodated larger P1′-substituents better than small and constrained ones.[22] In order to investigate if this might hold true also for our new inhibitors of class **A**, we decided to incorporate both phenylalanine and proline moieties, providing examples of a big P1′ side-chain and a small, rigidified P1′ group.

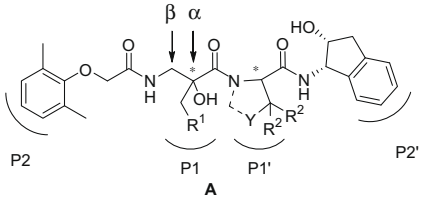

Figure 2. Generic structure **A** of the synthesized α-substituted norstatine inhibitors with variable length of the tether to the P1-phenyl group, variations in the P1′-group and two tunable stereocentra (*).

The specific objectives of this study were: (1) To identify adaptive inhibitors which are active against DV plasmepsins from all four infecting species. (2) To design and synthesize plasmepsin inhibitors devoid of any activity on hCatD. (3) To enhance the membrane permeability by altering the TS-mimicking secondary hydroxyl to a tertiary hydroxyl group by moving the P1-group from the β-position to the α-position in the norstatine TS mimic and by keeping the molecular weight below 650 g/mol. (4) To elucidate the impact of manipulating the stereochemistry of the thioproline and of the tertiary hydroxyl group with regard to activity on plasmepsins and selectivity profile. From a synthesis point of view, this would be the major challenge.

2. Results and discussion

2.1. Chemistry

The tertiary alcohol in the herein reported α-benzylnorstatines and α-phenylnorstatines originates from the epoxy acids **1a** or **1b**, respectively. The novel, four-step synthetic route to these key intermediates is outlined in Scheme 1. The acrylic acid **2a** was prepared by a Knoevenagel reaction, similar to the procedure previously reported for **2b**.[20] The reaction proceeded from the non-commercially available diacid, which was produced from diethyl 2-(phenethyl)malonate by an ester hydrolysis. Attempts to perform the epoxidation directly on **2a**,**b** were not successful. Thus, a fast and convenient one-pot microwave-heated (MW) protocol for esterification was developed, in order to generate the corresponding ethyl ester (**3a**,**b**). The esters were then readily oxidized by 3-chloroperbenzoic acid (*m*CPBA) to provide the epoxides **4a**,**b**. The building blocks, **1a**,**b**, were obtained by hydrolysis of the ester. This last step proved to be more successful using ethanolic KOH under dry conditions than using aqueous NaOH, thus avoiding concomitant epoxide opening by the hydroxide.

Two of the P1′ moieties, (*R*)- and (*S*)-5,5-dimethylthiazolidine (L- and D-Dmt), derive from the non-naturally occurring amino acids L- and D-Dmt carboxylic acid (**5**). They were synthesized, as described in Scheme 2, from L- and D-penicillamine (Pen), respectively, by a novel MW-assisted procedure inspired by the thiazoli-

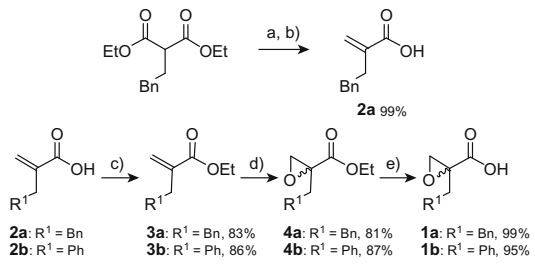

Scheme 1. Synthesis of the P1 moieties. Reagents and conditions: (a) NaOH, H_2O/THF/MeOH (1:2:1.2), reflux, 30 min; (b) HCHO (aq), $HNEt_2$, rt, 30 min then reflux, 3 h; (c) **2** or 2-benzylacrylic acid, $SOCl_2$, EtOH, 80 °C (MW), 5 min; (d) *m*CPBA, CH_2Cl_2, 18 h; (e) KOH (EtOH), rt, 15 min.

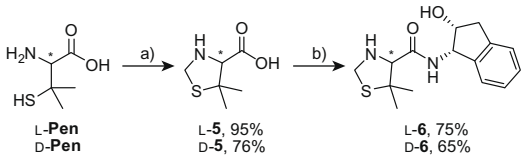

Scheme 2. Microwave-assisted synthesis of P1′P2′ structures encompassing Dmt. Reagents: (a) HCHO (aq), Pyr, 110 °C (MW), 5 min; (b) (1*S*,2*R*)-1-amino-2-indanol, HOBt, EDC, CH_2Cl_2, rt, 1–3 h.

dine-synthesis developed by Howard-Lock et al.[23] The elevated temperature (110 °C), provided by MW heating of the sealed reaction vial, resulted in a reduction of the reaction time from 16 h to 5 min.

The ring formation step was followed by a condensation reaction with (1*S*,2*R*)-1-amino-2-indanol, using HOBt and EDC as coupling reagents, furnishing (*R*)- and (*S*)-*N*-((1*S*,2*R*)-1-indanyl)-5,5-dimethylthiazolidine-4-carboxamide (L- and D-**6**) in 75% and 65% yields after silica flash chromatography. The nitrogen in the thiazolidine was not protected prior to the amidation, thus reducing the number of reaction steps by two. Although some dimer of Dmt could be detected in the reaction mixture, it was produced in very limited amounts according to LC–MS analysis.

The two other P1′P2′ motifs (L-**7** and L-**8**) were produced by the same coupling protocol from Boc-protected L-proline and Boc-protected L-phenylalanine with (1*S*,2*R*)-1-amino-2-indanol (Scheme 3). The amide coupling was quantitative in both cases, but due to problems in the work-up after the deprotection, the overall yields were merely 29% for L-**7** and 37% for L-**8**.

The next step in the synthesis was to couple the P1 epoxy acid with the P1′P2′ building block by a second amidation reaction, as depicted in Table 1. Due to the weak nucleophilic character of the Dmt-nitrogen, the amide couplings between **1a**,**b** and L- and D-**6** to yield epoxides **9–12** were extremely sluggish or did not work at all with a set of different coupling reagents, such as HOBt/EDC, HATU and PyBOP, used in various reaction media. Nevertheless, with PyAOP, the aza-analogue of PyBOP, in CH_2Cl_2 or DMF, the reactions proceeded reasonably well (Table 1), although full conversion of **6** was never realized, despite more than a week of stirring. The highest over-all yield for the amidation process was observed with the proline derivative L-**7** (62%). For the condensation between the less sterically hindered L-**8** and **1a**, PyBOP was used to afford epoxide **14**. After the condensation with the P1′P2′ moieties, complete epimeric separation of all the epoxides (**9–14**) was made possible with chromatography. The epoxy acid used in the reaction dictated which separation method had to be applied for successful separation of the diastereomers. When **1a** was used, epimeric separation was enabled by SP-HPLC equipped with a chiral column (Reprosil NR-R). This method, however, did not apply

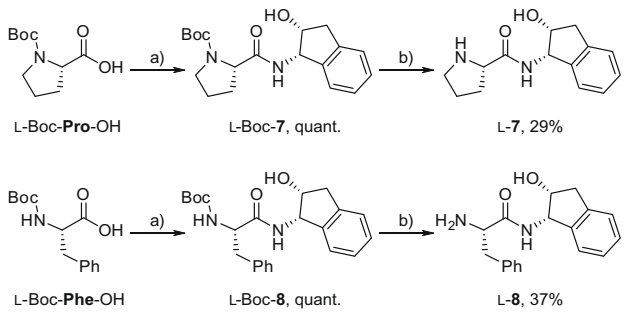

Scheme 3. Synthesis of P1′P2′ structures encompassing proline and phenylalanine. Reagents: (a) (1*S*,2*R*)-1-amino-2-indanol, HOBt, EDC, CH_2Cl_2, rt, 1 h; (b) HCl (4 M, 1,4-dioxane), rt, 5 h.

on the coupling products of **1b** and L- and D-**6**, where RP-HPLC equipped with a conventional C8 column proved to be superior.

The absolute configuration of the quaternary α-carbon in P1 of epoxide (*S*)-**11** was unambiguously established using X-ray crystallographic analysis of a crystal prepared from the corresponding inhibitor (*S*)-**17** in a saturated MeOH solution. The absolute configuration of (*S*)-**10** was determined by preparing the compound from enantiomerically pure (*S*)-**1a**, synthesized and optically characterized as previously reported.[20] The retention times on SP-HPLC and RP-HPLC of the two epimers of **10** were compared with the retention times for the diastereomerically pure (*S*)-epoxide. ^{1}H NMR and ^{13}C NMR experiments indicated that the analogous α-benzylnorstatine epimers (*S*)-**9** and (*R*)-**9** eluted with the same retention order on RP-HPLC as **10**, which corresponded to the reversed elution order on SP-HPLC (Reprosil NR-R column). Based on the NMR shifts and coupling constants and the results from chromatography experiments, the first eluted stereoisomer using SP-HPLC was assigned as (*R*)-**9** and the second eluted stereoisomer as (*S*)-**9**. ^{1}H NMR and ^{13}C NMR data and retention times on SP-HPLC and RP-HPLC of the corresponding inhibitors supported this hypothesis. A similar procedure was applied when establishing the absolute configuration of (*S*)-**12** and (*R*)-**12**, but then in comparison with the data of (*S*)-**11** and (*R*)-**11**. The two other epimeric pairs **13**,**14** were denoted (*A*) and (*B*) according to their elution order on SP-HPLC equipped with Reprosil NR-R column.

The diastereomerically pure epoxides **9–14**, were subsequently opened with a large excess of aqueous ammonia in methanol, providing the *N*-unsubstituted α-benzyl and α-phenylnorstatines as synthetic intermediates. The volatiles were evaporated in vacuo and the crude product was used without any further purification in the next step. The final inhibitors (**15–20**) were afforded by the condensation with the P2 group, 2-(2,6-dimethylphenoxy)acetic acid (**21**), which had been synthesized according to a literature procedure.[24] PyPOB was employed as coupling agent and di-*iso*-propyl-ethylamine (DIEA) as base. The stereopure inhibitors were isolated by RP-HPLC in 4–67% yield, as summarized in Table 2.

2.2. Enzyme inhibition

The twelve peptidomimetic structures **15**–**20** were evaluated for efficacy and selectivity by their ability to inhibit the paralogous enzymes PfPM2 and PfPM4, the orthologues of the latter, PmPM4, PoPM4, PvPM4, as well as hCatD. The results from the enzyme assays are presented as K_i values in Table 2.

Although only relatively minor structural modifications were made on this series of compounds compared to the lead structure KNI-10006 (Fig. 1), the drop in inhibitory activity on PfPM2, PfPM4 and hCatD was substantial. α-Phenylnorstatines (*S*)- and (*R*)-**16** was found to be more than 40,000 times less potent on PfPM2 than **KNI-10006**. This assay value suggests that the extra sterical congestion, caused by moving the P1 side-chain in the norstatine-scaffold from the β-carbon to the α-carbon, is not accepted by the enzyme. The corresponding α-benzylnorstatine analogue (*S*)-**15** was a moderately potent inhibitor of PfPM2 (K_i = 1.36 μM), a fact which might be explained by the increased flexibility of the P1 side-chain. Interestingly, the two most efficacious inhibitors of PfPM2 were (*S*)-17 (K_i = 0.44 μM) and (*S*)-18 (K_i = 0.83 μM), both featuring the new P1′ group D-Dmt and with (*S*)-configuration of the quaternary α-carbon in P1.

Generally, the affinities to PfPM4 were somewhat disappointing. With K_i values around 0.7 μM, compounds (*S*)- and (*R*)-**16** were the most potent inhibitors of PfPM4, an enzyme which clearly prefers α-phenylnorstatine (R1 = Ph) in the P1 position. The corresponding α-benzylnorstatine analogues (R1 = Bn), (*S*)- and (*R*)-**15**, were very moderate inhibitors with K_i values of 5.46 and 3.11 μM, respectively. The same trend could be deduced from the

Table 1
Synthesis and separation of the epimeric pairs of epoxides **9**–**14**

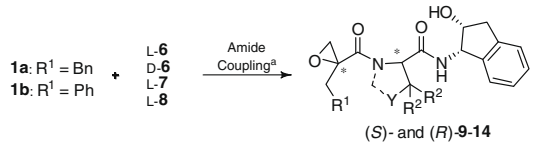

Cmpd	Y	R^1	R^2	From acid/amine	Coupling method[a]	Separation method[b]	Yield[c] (%)
(*S*)-**9**	SCH_2–	Bn	Me	**1a**/L-**6**	1	1	24
(*R*)-**9**	SCH_2–	Bn	Me	**1a**/L-**6**	1	1	25
(*S*)-**10**	SCH_2–	Ph	Me	**1b**/L-**6**	2	2	31
(*R*)-**10**	SCH_2–	Ph	Me	**1b**/L-**6**	2	2	45
(*S*)-**11**	SCH_2–	Bn	Me	**1a**/D-**6**	1	1	77
(*R*)-**11**	SCH_2–	Bn	Me	**1a**/D-**6**	1	1	49
(*S*)-**12**	SCH_2–	Ph	Me	**1b**/D-**6**	2	2	50
(*R*)-**12**	SCH_2–	Ph	Me	**1b**/D-**6**	2	2	34
(*A*)-**13**	CH_2CH_2–	Bn	H	**1a**/L-**7**	1	1	61
(*B*)-**13**	CH_2CH_2–	Bn	H	**1a**/L-**7**	1	1	62
(*A*)-**14**	CH_2Ph	Bn	H	**1a**/L-**8**	3	1	31
(*B*)-**14**	CH_2Ph	Bn	H	**1a**/L-**8**	3	1	29

[a] Coupling methods: (1) PyAOP, DIEA, in DCM, rt, 2–5 days; (2) As in (1), but in DMF; (3) PyBOP, DIEA, in DCM, rt, two days.
[b] Separation methods: (1) column chromatography (silica, EtOAc/*i*Hex) followed by SP-HPLC with a chiral column; (2) RP-HPLC with a C8 column.
[c] Isolated yields calculated from amine **6**–**8** with the assumption that **1** was a racemate. The maximum yield is thus 100%.

Table 2
Synthesis of inhibitors **15**–**20** and biochemical data with the best value of each enzyme indicated in bold[a]

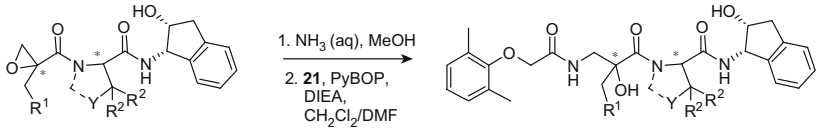

Cmpd	Structure	From epoxide	Yield[b] (%)	PfPM2[c] K_i (μM)	PfPM4 K_i (μM)	PmPM4[c] K_i (μM)	PoPM4[c] K_i (μM)	PvPM4[c] K_i (μM)	hCatD[c] K_i (μM)
(*S*)-**15**	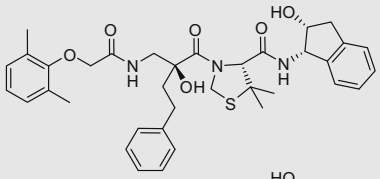	(*S*)-**9**	35	1.4	3.1	7.9	4.5	0.37	>10.0
(*R*)-**15**	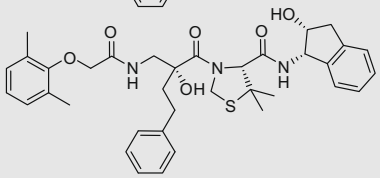	(*R*)-**9**	57	7.4	5.5	>20	6.5	2.2	>10.0
(*S*)-**16**	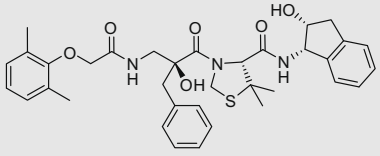	(*S*)-**10**	62	>20	**0.70**	0.26	**0.11**	0.16	>10.0
(*R*)-**16**	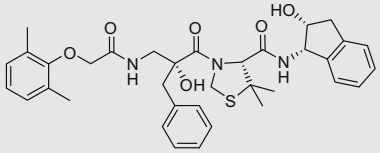	(*R*)-**10**	37	>20	**0.72**	0.25	0.53	0.19	>10.0
(*S*)-**17**	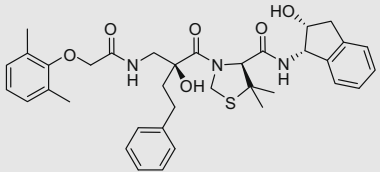	(*S*)-**11**	55	**0.44**	6.3	1.1	1.0	0.39	>10.0

Table 2 (*continued*)

Cmpd	Structure	From epoxide	Yield[b] (%)	PfPM2[c] K_i (μM)	PfPM4 K_i (μM)	PmPM4[c] K_i (μM)	PoPM4[c] K_i (μM)	PvPM4[c] K_i (μM)	hCatD[c] K_i (μM)
(*R*)-**17**	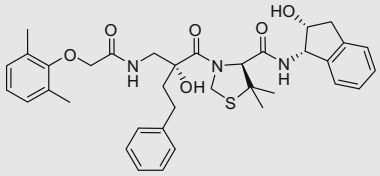	(*R*)-**11**	67	7.6	10.7	1.6	0.88	0.34	>10.0
(*S*)-**18**	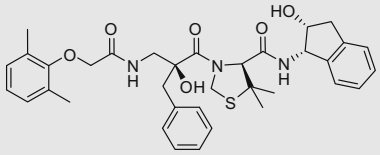	(*S*)-**12**	52	0.83	1.7	**0.21**	1.3	0.16	>10.0
(*R*)-**18**	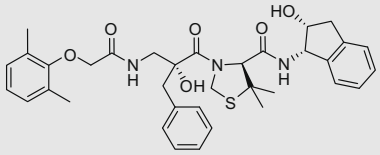	(*R*)-**12**	57	1.7	1.7	0.42	0.61	**0.12**	>10.0
(*A*)-**19**	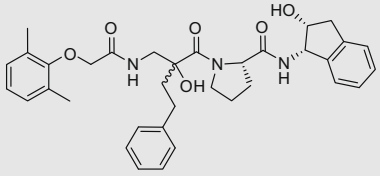	(*A*)-**13**	47	>20	30.2	14.5	7.2	2.2	>10.0
(*B*)-**19**	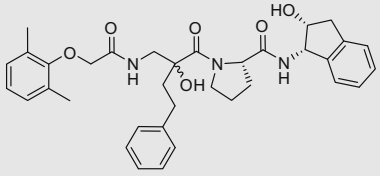	(*B*)-**13**	4	>20	26.9	13.0	10.3	1.3	n.d.
(*A*)-**20**	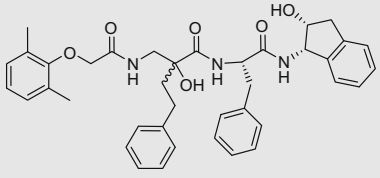	(*A*)-**14**	53	n.d.	>20	n.d.	n.d.	n.d.	>10.0
(*B*)-**20**	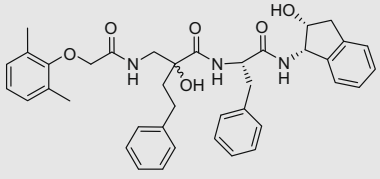	(*B*)-**14**	49	n.d.	>20	n.d.	n.d.	n.d.	>10.0

[a] R^1 = Bn or Ph, R^2 = Me or H, Y = SCH_2–, CH_2CH_2– or CH_2Ph.
[b] Isolated yield.
[c] n.d., not determined.

inhibitors incorporating the other stereoisomer in P1′, D-Dmt. Comparing the preference of the enzyme for the P1′ pseudoresidue, there was no significant difference between the pairs, but the overall tendency was that the compounds incorporating L-Dmt as P1′ were more active than the corresponding D-Dmt analogues (see epimers **15**/**16** and **17**/**18**). The impact of the absolute configuration of the TS-mimicking hydroxyl group was of subordinate importance for the inhibition efficacy on PfPM4.

There is no published inhibition data for PmPM4 of the parent compound, **KNI-10006**, but **KNI-764** (Fig. 1), encompassing identical P1 and P1′ groups, has a K_i value of 0.11 μm.[13] The potency of the best inhibitor of the α-substituted norstatines, (*S*)-18 (K_i = 0.21 μm), was found to be just barely lower. All four α-phenylnorstatines (**16** and **18**) were more active than the α-benzylnorstatines (**15** and **17**). In fact, the four α-phenylnorstatine diastereomers were more or less equipotent, regardless of the stereochemistry in either the P1′ or P1 position. On the other hand, with R1 = Bn in P1, D-configuration was preferred for the P1′ substituent.

The α-phenylnorstatine (*S*)-**16** was found to be the most active inhibitor of PoPM4. The K_i value of 0.11 μm represents the best potency in the entire series of new inhibitors, not only for PoPM4, but

for all the assessed enzymes. Compound (*S*)-**16** incorporated L-Dmt in P1′, which was the preferred P1′ motif for all α-phenylnorstatines. Nonetheless, if R1 = Bn, the compounds with D-configuration of the Dmt group ((*R*)- and (*S*)-**17**) were significantly more potent and the K_i values were ≤1 μM, compared to 6.5 μM and 4.5 μM for (*R*)- and (*S*)-**15**, respectively.

All tested inhibitors were active on PvPM4. It was also the enzyme that exhibited the least variation in the K_i data, ranging from 0.12 μM ((*R*)-**18**) to 2.2 μM ((*A*)-**19**). The α-phenylnorstatines were slightly more potent (K_i = 0.12–0.19 μM) than the α-benzylnorstatines, which also were active in the nanomolar range (K_i = 0.34–0.39 μM), except for compound (*R*)-**15** (K_i = 2.2 μM).

As depicted in Table 2, the l-Pro P1′ moiety found in (*A*)- and (*B*)-**19** was not well accommodated in any of the enzymes. The two compounds with L-Phe as P1′ motif ((*A*)- and (*B*)-**20**) were only tested on PfPM4, on which they were not active. Because of these negative results, they were not further evaluated on the other iso-enzymes.

None of the compounds were found to inhibit hCatD within measurable concentrations, which however was limited to 10.0 μM, due to the inherent fluorescence of the inhibitors. Yet, this series of compounds bound at least 5 000 times less strongly to hCatD than the lead compound **KNI-10006**. Inhibitor (*S*)-**16** exhibited more than a 14- to 90-fold selectivity for PM4 over hCatD and inhibitor (*S*)-**17** >20,000 times more active on PfPM2 than hCatD, compared to four times for **KNI-10006**. In addition, compounds (*S*)-**16**, (*R*)-**16**, (*S*)-**18**, (*R*)-**18**, (*A*)-**20** and (*B*)-**20** were assessed on the human aspartic protease drug-target β-amyloid converting enzyme (BACE-1), but none of them proved to be active in concentrations below 10 μm. This further confirmed our belief that this series of plasmepsin inhibitors do not affect human aspartic proteases to a considerable extent. Finally, all compounds, except for (*B*)-**19**, were also tested for their efficacy to inhibit HIV-1, either in an isolated protease assay or on an infected cell-line. Only (*R*)-**18** (K_i = 0.67 μM) and (*B*)-**20** (K_i = 1.0 μM) were active in the isolated protease assay, and (*S*)-**15** in the cell-based assay (EC_{50} = 6.4 μM).

From this dataset of measured K_i values in Table 2 some general trends can be deduced: (1) There was no significant correlation between the efficacy for which the compounds inhibit PfPM2 and PfPM4 or its orthologues. Similar patterns have previously been observed both for compounds of pseudopeptidic character[12,22,25] and for more drug-like peptidomimetics.[8] (2) The α-phenylnorstatines were stronger inhibitors of the four PM4 than the α-benzylnorstatines. (3) The presence of D-Dmt in P1′ reduced the influence of the structural characteristics of P1 on the inhibition of PM4 orthologues in Po, Pv and Pm. Thus, neither an alteration of the length of the tether nor the stereochemistry of the α-carbon in P1 resulted in a change of the K_i values. In comparison, the compounds encompassing L-Dmt demonstrated a greater variation in potency depending on the character of the P1 moiety.

2.3. Computational evaluation

As an attempt to explain the considerably lower affinities to PfPM4 experienced for the α-phenylnorstatines compared to the lead structure **KNI-10006**, several computational methods were employed. An exhaustive docking search was conducted, followed by molecular dynamics (MD) and binding affinity estimations. This computational protocol has been proven successful in the design of other plasmepsin inhibitors.[26]

Even if the binding orientation of **KNI-764** in PmPM4 has been elucidated by X-ray crystallography (PDB entry 2ANL)[13] (Fig. 3, binding mode 1) and shown to explain the differences in affinity for a series of **KNI** compounds,[27] other alternative binding modes of norstatine-based compounds have been proposed recently

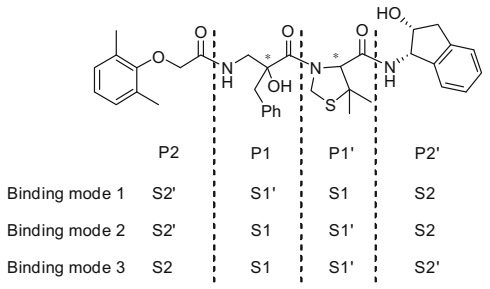

Figure 3. Proposed binding orientations of the herein reported α-phenylnorstatines in the binding site of PM4 enzymes.

(e.g., binding mode 3 in Fig. 3).[28] Additionally, the binding mode of (*R*)-phenylnorstatines to HIV-1 protease was found to differ in the H-bond pattern of the TS-mimic as compared to (*S*)-derivatives, such as **KNI** compounds.[29] Therefore, we felt encouraged to investigate the binding poses of the newly designed compounds with an α-phenylnorstatine scaffold (i.e., R = Ph in Table 2). The four inhibitors (*S*)-**16**, (*R*)-**16**, (*S*)-**18** and (*R*)-**18** were systematically docked into the active site of PmPM4, the enzyme of choice since the crystal structure is pre-arranged to bind norstatine inhibitors. The binding affinity estimations were instead conducted on PfPM4, which allowed us to compare the results with previously experimentally[17] and computationally[27] determined data for **KNI-10006**.

The docking results into PmPM4 indicated that only one binding orientation could be considered for compounds (*R*)-**16** and (R)-**18** (binding mode 1, Fig. 3). This binding mode corresponds to the orientation of KNI-764, observed by the X-ray crystallography in PmPM4,[13] and modeled for **KNI-10006**.[10,27] Conversely, two different binding orientations were isolated from the docking runs of the two (*S*)-α-phenylnorstatines ((*S*)-**16** and (*S*)-**18**), featuring the opposite absolute configuration of the TS mimic. The first orientation is analogous to the binding mode (1) (Fig. 3), as discussed before for the (*R*)-α-phenylnorstatines and also for the parent phenylnorstatine **KNI** compounds, whereas the second positioning involves an alternative binding mode which was more frequently observed for the two compounds considered, (*S*)-**16** and (*S*)-**18** (binding mode 2 in Fig. 3). In this second orientation, the P1 and P1′ inhibitor side chains interchange their positions in the corresponding S1 and S1′ binding pockets, with respect to the binding mode experimentally observed for **KNI-764**.

In order to gain more knowledge about the ligand-protein interactions and to choose between the two possible binding modes observed for the compounds with (*S*)-α-phenylnorstatines, an MD simulation was performed for every binding pose selected at the docking stage, as bound to PfPM4. Additionally, we considered manual docking as starting pose for the MD simulation for every compound in two alternative orientations. In the first orientation, the compounds were built on the basis of **KNI-764** as found in the 2ANL structure (binding mode 1). This conformation could only be accomplished for the (*R*)-α-phenylnorstatines. The second orientation is depicted in binding mode (3) (Fig. 3), and corresponds to a totally inverted binding orientation relative to the binding mode (1). Even if this binding mode was not found in the docking runs, we considered this orientation since other authors had suggested that alternate binding orientations could exist for different **KNI** inhibitors.[28] Between two and six binding poses per inhibitor were simulated, providing a total of 20 starting poses for further evaluation.

Binding affinities were systematically calculated by the linear interaction energy method (LIE) and the most energetically favored binding pose of each molecule ((*S*)-**16**, (*R*)-**16**, (*S*)-**18** and (*R*)-**18**), is shown in Table 3. Although we did not attempt to explain the abso-

Table 3
Experimental and calculated energetics (kcal/mol) of PfM4 inhibition of the four α-phenylnorstatines under study and a β-phenylnorstatine, **KNI-10006**

Cmpd	ΔG_{bind}, exp (kcal/mol)	ΔG_{bind}, LIE (kcal/mol)	Ligand–surrounding interactions (kcal/mol)			
			$\langle V_{l-s}^{vdw}\rangle_p$	$\langle V_{l-s}^{el}\rangle_p$	$\langle V_{l-s}^{vdw}\rangle_w$	$\langle V_{l-s}^{el}\rangle_w$
(*R*)-**16**	−8.44	−4.57 ± 0.4	−76.7 ± 1.1	−68.6 ± 0.3	−−49.3 ± 0.1	−68.6 ± 0.3
(*S*)-**16**	−8.45	−5.71 ± 0.5	−82.2 ± 1.2	−69.6 ± 0.1	−49.1 ± 0.1	−70.4 ± 0.7
(*R*)-**18**	−7.92	−5.56 ± 0.8	−83.2 ± 0.1	−73.0 ± 0.9	−48.9 ± 0.4	−74.9 ± 1.4
(*S*)-**18**	−7.92	−8.99 ± 0.3	−81.3 ± 0.1	−80.1 ± 0.3	−48.1 ± 0.3	−72.0 ± 0.5
KNI-10006[a]	−10.7	−14.1 ± 0.4	−77.2 ± 0.1	−93.3 ± 0.7	−42.9 ± 0.0	−69.4 ± 0.6

[a] Data reported by Gutierrez-de-Teran et al.[27]

lute binding affinities in our calculations, the equipotency of the compound series was relatively correctly reproduced, apart from the overestimation of the calculated affinity of compound (*S*)-**18**. The data for compound **KNI-10006** have been included for comparison.[27] For all four α-phenylnorstatines, the ligand binding affinity was found mainly to be due to nonpolar contributions, which indicated that polar interactions generally just counterbalanced desolvation, except in the case of compound (*S*)-**18** where they favor binding to the enzyme. In contrast, for the phenylnorstatines, that is, the **KNI** compounds, previous studies have shown that both polar and nonpolar contributions account for the comparatively stronger ligand binding.[27] Thus, these results suggest that the introduction of the α-substituent in the norstatine scaffold impairs the strong polar interactions of the catalytic aspartates with the TS-mimicking hydroxyl and the central P1 carbonyl group, previously observed with norstatine-containing plasmepsin inhibitors.

The binding affinity calculations indicated that inhibitors (*R*)-**16** and (*R*)-**18** should bind to PfPM4 according the binding mode 1, as suggested at the docking stage (Fig. 4a and b), whereas for the inhibitors with the (*S*)-configuration at the TS mimic ((*S*)-**16**, (*S*)-**18**), binding mode (2) was the most favored one (Fig. 4c and d). The third possibility, binding mode (3) (Fig. 3), showed least favored binding affinity estimates for the four studied compounds, hence it was disregarded for further consideration. A detailed analysis of the ligand binding interactions followed in order to understand the reduced affinity with respect to the original norstatine scaffold in **KNI-10006**. Interestingly, the configuration of the thioproline pseudoresidue in P1′ (L or D) exerted a great influence on the orientation of the two carbonyl oxygens adjacent to it. Compound (*R*)-**16**, with the same absolute configuration in P1′ as the **KNI** compounds, showed the most conserved binding pose with respect to **KNI-10006** (Fig. 4a). The main difference was found in the H-bond network with the catalytic aspartates (Asp34 and Asp214). The TS-mimicking α-hydroxyl interacted with Asp34 while the P1 carbonyl adjacent to it pointed in the opposite direction. In fact, the interaction with the catalytic aspartates resembled the conforma-

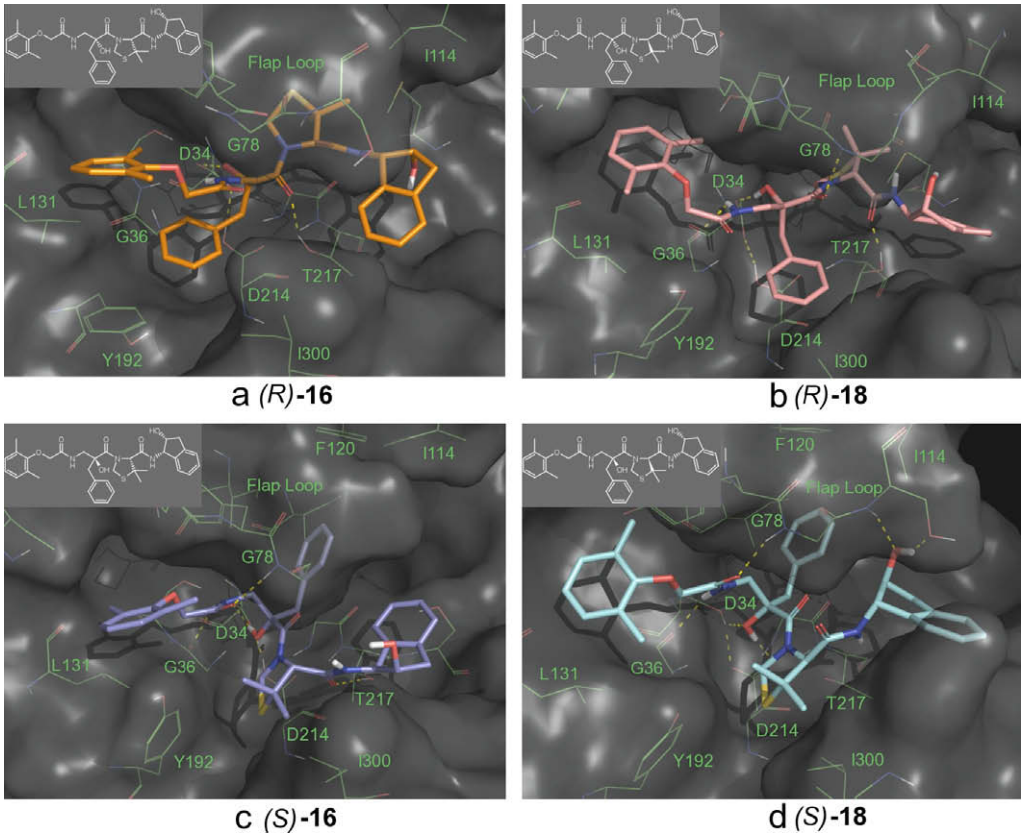

Figure 4. Structures of four PfPM4 enzyme–inhibitor complexes, as average coordinates of the MD trajectories sampled for binding free energy calculations. The enzyme is depicted with the prime side subsites to the left and the non-prime subsites to the right. From top, left corner: (a) (*R*)-**16** in orange, (b) (*R*)-**18** in pink, (c) (*S*)-**16** in purple, (d) (*S*)-**18** in cyan. Yellow dashed lines indicate frequently observed hydrogen bonds.

tion of the (*R*)-phenylnorstatine derivative crystallized with HIV-1 protease by Brynda el al.[29] In our simulations, this carbonyl was interacting with Thr217 in the S1 subsite, as depicted in Figure 4a. Inhibitor (*R*)-**18**, with the inverse configuration in P1′, that is, D-Dmt, exhibited the same binding pose in the prime subsites, whereas the conformation of the P1′P2′ pseudoresidues in the non-prime sites of the enzyme was slightly altered (Fig. 4b). Nevertheless, the H-bond network was satisfied with the P1 carbonyl interacting with Gly76 at the tip of the flap and the P1′ carbonyl with Thr217. For the two (*S*)-α-phenylnorstatines, the binding mode in the S2′ site was well conserved with respect to **KNI-764**, while major differences were discovered in the other three pockets. The two compounds had the carbonyl at P1 pointing towards the tip of the flap and, depending on the configuration of the thioproline, the carbonyl in P1′ pointing towards the inner part of the enzyme, interacting with Thr217 (P1′ = L-Dmt, (*S*)-**16**) or also towards the flap (P1′ = D-Dmt, (*S*)-**18**) as depicted in Figure 4c and d, respectively.

3. Conclusions

A new class of plasmepsin inhibitors encompassing an α-substituted norstatine TS-isostere scaffold was prepared. Variations of the P1′ pseudoresidue and alterations of the stereochemistry and the size of the P1 α-substituent provided twelve stereopure α-phenylnorstatine and α-benzylnorstatine test compounds. The investigation afforded a handful of drug-like inhibitors of Pf-, Pm-, Po- and PvPM4, with not only K_i values in the nanomolar range, but also with high selectivity versus the human aspartic proteases hCatD and BACE-1. Furthermore, the incorporation of the D-Dmt motif in the inhibitors furnished a reduced sensitivity for structural modifications of the α-substituent in the norstatine core, that is, the length of the P1 tether and the absolute configuration of the α-carbon. However, the best over-all inhibitor of PM4 was LL-Dmt comprising (*S*)-**16** (K_i = 0.70, 0.26, 0.11 and 0.16 μM on Pf, Pm, Po and Pv, respectively), and with a more than 90- to 14-fold selectivity over hCatD. Note that the importance of the absolute configuration of the α-carbon seems to be very small, as proven by the almost equipotent PM4 inhibition profile experienced with epimeric (*R*)-**16**.

Although the new inhibitors were most active in the PM4 orthologue assays, two D-Dmt based compounds ((*S*)-**17** and (*A*)-**18**) accounted for relatively good inhibitory potency against PfPM2 (K_i = 0.44 μM and 0.88 μM, respectively). Hence, the D-Dmt moiety was identified as a new promising P1′ residue in the active site also of PfPM2, being more potent compared than the 'natural' L-Dmt motif. Being highly active in all five malaria enzyme assays, D-Dmt containing α-phenylnorstatine (*S*)-**18** can be stated as the most adaptive inhibitor in the whole series.

The observed loss of affinity to PfPM4, due to the move of the P1 substituent to the α-position in the norstatine scaffold, as compared to the β-substituted lead compound, **KNI-10006**, could be explained by less favorable polar interactions with the enzyme. In addition, a comprehensive computational exploration of the binding poses of this novel class of α-phenylnorstatine derivatives to PmPM4 and PfPM4 was carried out. The computational results suggested that the compounds with the (*R*) configuration of the TS-mimicking P1 present the same binding orientation as observed for **KNI-764**, whereas the compounds with an inverted (*S*) configuration interchange the position of the P1 and P1′ substituents in their respective S1/S1′ binding pockets.

To the best of our knowledge, there are presently only three publications available reporting inhibitors of all four orthologues of PM4.[12,22,30] The structures included there are all large and of pseudopeptidic character. Thus, the α-substituted norstatine structures reported in this contribution are the first drug-like peptidomimetic compounds which have been tested and proven to be efficient inhibitors in the nanomolar range of the PM4 iso-enzymes. It can be stated, in general terms, that the inhibitors of PfPM4 are active also on the DV plasmepsins of the other species. Nonetheless, despite the small differences in the active sites of the four PM4, variations in inhibitory activity were revealed. For example, compound (*R*)-**17** was found to be a weak inhibitor of PfPM4, but provided sub-micromolar activities on both PoPM4 and PvPM4, thus showing a >30-fold deviation depending on the enzyme orthologue. Therefore, we believe it is important to measure the inhibitory effect of new inhibitors in all four PM4 enzymes. The experimental and computational information reported herein might have implications for future design of new PM4 inhibitors.

4. Experimental

4.1. Chemistry

4.1.1. General information

The microwave experiments were conducted using Emrys Initiator™ or Smith Synthesizer™ single mode cavity, producing controlled irradiation at 2450 MHz in sealed reaction vials (capable of withholding elevated pressure) dedicated for microwave processing, under air and with magnetic stirring. The temperature of the reaction mixture was measured using a built-in, on-line infrared temperature sensor. For column chromatography commercially available Silica Gel 60 (particle size: 0.040–0.063 mm) was used. Analytical thin layer chromatography was done using glass sheets precoated with Silica Gel 60 F_{254} and visualization of components was made by UV, I_2 and/or Pancaldi's solution followed by heating. Analytical HPLC–MS was performed on a Gilson–Finnegan ThermoQuest AQA system equipped with a C18 (Onyx Monolithic C18 (50 × 4.6 mm)) column, using CH_3CN in 0.05% aqueous HCOOH as mobile phase at a flow rate of 4 mL/min with UV (214 and 254 nm) and MS (ESI^+ or ESI^-) detection. HPLC–MS was complemented with RPLC on a Gilson HPLC Pump 312 system with a LKB variable wavelength detector equipped with a C8 (Agilent Zorbax SB-C8 (5 μm, 50 × 4.6 mm)) column, using CH_3CN in 0.05% aqueous HCOOH or 0.10% aqueous TFA as mobile phase at a flow rate of 2 mL/min with UV (220 nm) detection. Preparative RP–HPLC was performed on a Gilson HPLC Pump 312 with a LKB system variable wavelength detector equipped with a C8 (Agilent Zorbax SB-C8 (5 μm, 50 × 21.2 mm)) column, using CH_3CN in 0.05% aqueous HCOOH or 0.10% aqueous TFA as mobile phase at a flow rate of 5 mL/min with UV (220 or 230 nm) detection. Specific rotations (α_D) are reported in deg/dm and the concentration (*c*) is given as g/100 mL in the specified solvent. ^1H and ^{13}C NMR spectra were recorded on Varian Mercury Plus instruments at 24 °C, ^1H NMR spectra were recorded at 399.9 MHz and ^{13}C NMR spectra at 100.5 MHz. The chemical shifts for ^1H NMR and ^{13}C NMR were referenced to TMS via the solvent signals (^1H NMR at 7.26 ppm for $CDCl_3$ and at 3.31 for CD_3OD and ^{13}C NMR at 77.16 for $CDCl_3$ and 49.00 for CD_3OD). Exact molecular masses (HRMS) were determined on Micromass Q-Tof2 mass spectrometer equipped with an electrospray ion source. Analytische Laboratorien, Lindlar, Germany and Microkemi, Uppsala, Sweden, performed elemental analyses. The crystallization and X-ray determination of inhibitor (*S*)-**17** were performed at the Latvian Institute of Organic Synthesis, Latvia, Riga. CCDC724531 contain the Supplementary crystallographic data for this paper. These data can be obtained free of charge from The Cambridge Crystallographic Data Centre via www.ccdc.cam.ac.uk. The purity for all new compounds were established to be ≥98% by at least two HPLC systems, ^1H NMR, ^{13}H NMR and elemental analysis or HRMS. All starting materials,

reagents and solvents were purchased from commercial suppliers and were used directly as received. Compounds **2b**[31] and **21**[24] were synthesized according to literature procedures.

4.1.2. Experimental details and spectroscopic data for compounds 1a,b–4a,b

Compound **2a** is essentially synthesized according to a literature procedure for the benzyl analogue **2b**.[20,31] Compounds **3a**[32] and **4a**[33] are known from the literature, but the microwave-assisted esterification is a new procedure resulting in a higher yield. There are no previously reported spectroscopic data for **3a** and **4a**. The synthesis of enantiomerically pure epoxy acid **1b** is described in the literature,[20] but results in a lower over-all yield (58%) compared to the racemic method described herein (71%).

4.1.2.1. 2-Methylene-4-phenylbutyric acid (2a). NaOH (10.40 g, 260 mmol) was dissolved in water (25.0 mL) and diethyl 2-(phenylethyl)malonate (13.09 g, 49.53 mmol), THF (50.0 mL) and MeOH (30.0 mL) were added. The reaction mixture was refluxed under stirring for 30 min. The solvents were evaporated under vacuum and the residue was dissolved in water (400 mL) and acidified to pH <1 by addition of 2 M HCl (aq). The reaction mixture was extracted with EtOAc (3 × 250 mL). The combined organic phases were dried over $MgSO_4$, filtered and evaporated to yield phenylethyl malonic acid (10.5 g, quantitative) as a white solid. The product was used without any further purification in the next step. MS-ESI$^-$: *m/z* 207, $[M–H]^+$. Phenylethyl malonic acid (10.4 g, 49.5 mmol) was mixed with aqueous formaldehyde (37% wt, 22.0 mL, 290 mmol) and diethylamine (57 mL, 55 mmol) was added dropwise. The reaction mixture was stirred at rt for 30 min until a white solid was formed and then refluxed for 3 h. The reaction mixture was reduced under vacuum, acidified with 5 M HCl (aq) and extracted with EtOAc (3 × 100 mL). The combined organic phases were dried over $MgSO_4$, filtered, evaporated and dried under vacuum over-night to yield **2a** (8.728 g, 99%) as a off-white solid. ^{1}H NMR (400 MHz, $CDCl_3$): δ = 7.33–7.13 (m, 5H, Ar), 6.32 (s, 1H), 5.62 (s, 1H), 2.84 (d, *J* = 7.2 Hz, 1H), 2.82 (d, *J* = 5.6 Hz, 1H), 2.64 (d, *J* = 5.6 Hz, 1H), 2.62 ppm (d, *J* = 7.2 Hz, 1H); ^{13}C NMR (100 MHz, $CDCl_3$): δ = 172.4, 141.4, 139.4, 128.6, 128.5, 128.0, 126.2, 34.9, 33.7 ppm; MS-ESI$^-$ (*m/z* 175, $M–H^+$).

4.1.2.2. 2-Methylene-4-phenylbutyric acid ethyl ester (3a).[32] Compound **2a** (3.01 g, 17.08 mmol) and thionylchloride (1.6 mL, 22 mmol) were stirred for 2 min in a capped 10–20 mL Emrys reaction vial. Absolute EtOH (10.00 mL) was added dropwise with a syringe. The reaction mixture was irradiated with microwaves for 5 min at 80 °C. Another 1.6 mL (22 mmol) thionylchloride was added by syringe and the vial was irradiated for an additional 5 min at 80 °C. The reaction mixture was reduced under vacuum, diluted with EtOAc (150 mL), washed with saturated $NaHCO_3$ (aq) (3 × 50 mL), 0.5 M HCl (aq) (50 mL) and brine. The organic phase was reduced and purified (silica, EtOAc/*i*Hex, 1:20) to yield **3a** (2.895 g, 83%) as a clear oil. ^{1}H NMR (400 MHz, $CDCl_3$): δ = 7.32–7.26 (m, 2H), 7.22–7.17 (m, 3H), 6.17–6.16 (m, 1H), 5.55 (dd, *J* = 2.7, 1.4 Hz, 1H), 4.23 (q, *J* = 7.2 Hz, 2H), 2.82 (d, *J* = 7.2 Hz, 1H), 2.79 (d, *J* = 5.6 Hz, 1H), 2.64 (d, *J* = 5.6 Hz, 1H), 2.62 (d, *J* = 7.2 Hz, 1H), 1.32 ppm (t, *J* = 7.2 Hz, 3H); ^{13}C NMR (100 MHz, $CDCl_3$): δ = 167.3, 141.6, 140.3, 128.6, 128.5, 126.1, 125.2, 60.8, 35.1, 34.1, 14.4 ppm; MS-ESI$^+$: *m/z* 205, $[M+H]^+$.

4.1.2.3. 2-Benzylacrylic acid ethyl ester (3b). Compound **3b** was prepared according to the procedure for compound **3a** using **2b** (1.00 g, 6.17 mmol) and thionylchloride (1.5 + 0.5 mL, 21 + 7 mmol) to yield **3b** (1.00 g, 86%) as a clear oil.

4.1.2.4. 2-Phenethyloxirane-2-carboxylic acid ethyl ester (4a).[33] Compound **3a** (4.00 g, 19.60 mmol) was dissolved in CH_2Cl_2 (275 mL) and *m*CPBA (77% in balance with 3-chlorobenzoic acid and water, 48.240 g, 195.7 mmol) was added. The reaction mixture was refluxed under stirring. After 4 h, additional *m*CPBA (10.0 g, 40.0 mmol) was added and the mixture refluxed for another 14 h. The reaction mixture was washed with 10% $Na_2S_2O_3$ (aq), sat HCO_3 (aq) (4 × 150 mL), reduced under vacuum and purified (silica, EtOAc/*i*Hex, 1:20–1:2). to yield **4a** as an uncolored syrup (3.487 g (81%). ^{1}H NMR (400 MHz, $CDCl_3$): δ = 7.32–7.26 (m, 2H), 7.22–7.17 (m, 3H), 4.23 (dd, *J* = 10.8, 7.2 Hz, 1H), 4.20 (dd, *J* = 10.8, 7.2 Hz, 1H), 3.05 (d, *J* = 5.9 Hz, 1H), 2.84–2.79 (m, 2H), 2.77 (d, *J* = 5.9 Hz, 1H), 2.43–2.33 (m, 1H), 2.06–1.86 (m, 1H), 1.30 ppm (t, *J* = 7.2 Hz, 3H); ^{13}C NMR (100 MHz, $CDCl_3$): δ = 170.3, 141.1, 128.6, 128.5, 126.3, 61.8, 56.7, 52.3, 33.5, 31.3, 14.2 ppm; MS-ESI$^+$: *m/z* 221, $[M+H]^+$.

4.1.2.5. 2-Benzyloxirane-2-carboxylic acid ethyl ester (4b). Compound **4b** was prepared according to the procedure for compound **4a** using **3b** (1.40 g, 7.36 mmol) and *m*CPBA (8.47 g, 36.8 mmol) to yield **4b** (1.32 g, 87%) as an uncoloured syrup.

4.1.2.6. 2-Phenethyloxirane-2-carboxylic acid (1a). Compound **4a** (2.05 g, 9.29 mmol) was dissolved in EtOH (13 mL) and freshly prepared 1.22 M ethanolic KOH (13.0 mL, 15.9 mmol) was added under vigorous stirring. The reaction mixture was stirred at room temperature and after 15 min a white solid was formed. The reaction mixture was diluted with satd $NaHCO_3$ (5 mL), acidified with 5 M HCl (aq) to pH 8, washed with EtOAc (3 × 75 mL), acidified to pH <1 by addition of 5 M HCl (aq) and extracted with EtOAc (3 × 150 mL). The combined organic phases were dried over $MgSO_4$, filtered and evaporated to yield **1a** as a pale yellow syrup (1.763 g, 99 %): ^{1}H NMR (400 MHz, $CDCl_3$): δ = 7.33–7.27 (m, 2H), 7.23–7.18 (m, 3H), 3.11 (d, *J* = 5.7 Hz, 1H), 2.87 (d, *J* = 5.7 Hz, 1H), 2.85–2.81 (m, 2H), 2.43–2.33 (m, 1H), 2.06–1.86 ppm (m, 1H); ^{13}C NMR (100 MHz, $CDCl_3$): δ = 175.1, 140.8, 128.7, 128.5, 126.4, 56.6, 52.6, 33.0, 31.2 ppm; MS-ESI$^-$: *m/z* 191, $[M–H]^+$. Anal. Calcd for $C_{11}H_{12}O_3 \cdot 1/4H_2O$: C, 61.16; H, 6.40. Found: C, 67.0; H, 6.4.

4.1.2.7. 2-Benzyloxirane-2-carboxylic acid (1b).[20] Compound **1b** was prepared according to the procedure for compound **1a** using **4b** (1.30 g, 6.30 mmol) and 1.22 M ethanolic KOH (11 mL, 13.4 mmol) to yield **1b** (1.15 g, 95%) as thick paste.

4.1.3. Experimental details and spectroscopic data for compounds L-5, D-5, L-6, D-6, 7 and 8

The synthesis of compounds L-**5** and D-**5**, are described in the literature but with a lower isolated yield.[23] The synthesis of the *N*-Boc derivative of compound L-**6** is described in the literature.[34] The syntheses of **7**[35], **8** and Boc-**8**[36] are reported in the literature, but with alternative procedures. The spectroscopic data of the known substances matched with the literature, when reported, otherwise we have reported the data below. Analytical SP-HPLC of L-**6** and D-**6** was performed on a Gilson HPLC Pump 312 with LKB system variable wavelength detector equipped with a (Reprosil Chiral NR-R (8 μm, 250 × 4.6 mm)) column, using *i*PrOH in *i*Hex as mobile phase at a flow rate of 2 mL/min with UV (220 nm) detection.

4.1.3.1. (*R*)-5,5-Dimethyl-1,3-thiazolidine-4-carboxylic acid (L-5). L-Penicillamine (0.50 g, 3.50 mmol) was suspended in 1.50 mL aqueous formaldehyde (37% wt, 20.0 mmol), three drops of pyridine and 2.5 mL ethanol in a 2–5 mL Emrys reaction vial. The vial was irradiated by microwaves for 5 min (hold-time) at 110 °C. After cooling for >1 h, the product had crystallized and could be filtered off and washed with cold Et_2O to give compound L-**5** as white crystals (0.516 g, 95%). MS-ESI$^+$: *m/z* 162, $[M+H]^+$.

4.1.3.2. (*S*)-5,5-Dimethyl-1,3-thiazolidine-4-carboxylic acid (D-5). Compound D-**5** was synthesized by the same procedure as L-**5** from D-penicillamine (0.50 g 3.50 mmol), but 2 mL Et_2O was added to the reactions vial after MW-irradiation and cooling to rt, in order to initiate the crystallization. The product, D-**5** was isolated as white crystals (0.412 g, 76%). MS-ESI$^+$: *m/z* 162, $[M+H]^+$.

4.1.3.3. (*R*)-*N*-((1*S*,2*R*)-2-Hydroxy-1-indanyl)-5,5-dimethylthiazolidine-4-carboxamide (L-6). Carboxylic acid L-**5** (0.454 g, 2.82 mmol) and (1*S*,2*R*)-1-amino-2-indanol (0.511 g, 3.43 mmol), EDC (0.602 g, 3.14 mmol), HOBT (0.425 g, 3.14 mmol) were stirred in dry CH_2Cl_2 (20 mL) for 3 h at rt. The reaction mixture was concentrated and purified (silica, 2% MeOH in CH_2Cl_2) to give L-**6** (0.608 g, 75%) as a white solid. Compound L-**6**: t_R = 5.49 min (SP-HPLC, 15% *i*PrOH in *i*Hex); $[\alpha]_D^{22} = -31.4$ (*c* 0.98, MeOH: CH_2Cl_2 (15:1)); ^{1}H NMR (400 MHz, CD_3OD): δ = 7.29–7.17 (m, 4H), 5.36 (d, *J* = 5.4 Hz, 1H), 4.54 (dt, *J* = 5.4, 2.6 Hz, 1H), 4.31 (d, *J* = 9.4 Hz, 1H), 4.14 (d, *J* = 9.4 Hz, 1H), 3.57 (s, 1H), 3.15 (dd, *J* = 16.3, 5.4 Hz, 1H), 2.94 (dd, *J* = 16.3, 2.6 Hz, 1H), 1.68 (s, 3H), 1.38 ppm (s, 3H); ^{13}C NMR (100 MHz, CD_3OD): δ = 171.4, 142.2, 141.8, 129.1, 127.9, 126.2, 125.5, 75.4, 73.8, 58.3, 57.9, 51.5, 40.8, 29.1, 28.1 ppm; MS-ESI$^+$: *m/z* 293, $[M+H]^+$.

4.1.3.4. (*S*)-*N*-((1*S*,2*R*)-2-Hydroxy-1-indanyl)-5,5-dimethylthiazolidine-4-carboxamide (D-6). Carboxylic acid D-**5** (0.335 g, 1.24 mmol) and (1*S*,2*R*)-1-amino-2-indanol (0.301 g, 1.87 mmol), EDC (0.395 g, 2.06 mmol), HOBT (0.278 g, 2.06 mmol) were stirred in dry CH_2Cl_2 (20 mL) for 1 h at rt. The reaction mixture was concentrated and purified (silica, 3% MeOH in CH_2Cl_2) to give D-**6** (0.354 g, 65%) as a white solid. Compound D-**6**: t_R = 4.73 min (SP-HPLC, 15% *i*PrOH in *i*Hex); $[\alpha]_D^{22}$ = +53.6 (*c* 1.37, MeOD); ^{1}H NMR (400 MHz, CD_3OD): δ = 7.29–7.20 (m, 4H), 5.32 (d, *J* = 5.2 Hz, 1H), 4.59 (dt, *J* = 5.2, 2.0 Hz, 1H), 4.34 (d, *J* = 9.3 Hz, 1H), 4.15 (d, *J* = 9.3 Hz, 1H), 3.56 (s, 1H), 3.16 (dd, *J* = 16.4, 5.2 Hz, 1H), 2.94 (dd, *J* = 16.4, 2.0 Hz, 1H), 1.67 (s, 3H), 1.39 ppm (s, 3H); ^{13}C NMR (100 MHz, CD_3OD): δ = 171.6, 141.99, 141.96, 129.1, 127.9, 126.3, 125.1, 75.2, 73.9, 58.9, 57.9, 51.7, 40.6, 29.3, 28.2 ppm; MS-ESI$^+$: *m/z* 293, $[M+H]^+$.

4.1.3.5. (*S*)-1-(*tert*-Butoxycarbonyl)-*N*-((1*S*,2*R*)-2-hydroxy-1-indanyl)pyrrolidine-5-carboxamide (Boc-7). Boc-(*S*)-proline (1.01 g, 4.67 mmol) and (1*S*,2*R*)-1-amino-2-indanol (0.837 g, 5.613 mmol), PyBOP (2.673 g, 5.136 mmol), DIEA (1.60 mL, 9.346 mmol) were stirred in dry CH_2Cl_2 (80 mL) for 3 h at rt. The reaction mixture was concentrated and purified (silica, EtOAc/*i*Hex, 1:1–5:1) to give Boc-**7** (1.62 g, quantitative) as a white solid. ^{1}H NMR (400 MHz, CD_3OD): δ = 7.31–7.16 (m, 4H), 5.33–5.24 (m, 1H), 4.55 (s, 1H), 4.37–4.30 (m, 1H), 3.57–3.48 (m, 1H), 3.48–3.39 (m, 1H), 3.14 (dd, *J* = 16.4, 5.1 Hz, 1H), 2.97–2.88 (m, 1H), 2.34–2.18 (m, 1H), 2.18–2.06 (m, 1H), 2.06–1.86 (m, 2H), 1.43 ppm (s, 9H); ^{13}C NMR (100 MHz, CD_3OD): δ = 175.7, 175.3, 142.2, 141.6, 129.0, 127.7, 126.1, 125.4, 81.6, 79.1, 73.6, 61.7, 58.5, 47.8, 32.6, 28.7, 24.6 ppm; MS-ESI$^+$: *m/z* 347, $[M+H]^+$.

4.1.3.6. (*S*)-*N*-((1*S*,2*R*)-2-Hydroxy-1-indanyl)pyrrolidine-5-carboxamide (7). Compound Boc-**7** (0.730 g, 2.11 mmol) was dissolved in dioxane (11 mL) and 4 M HCl (1,4-dioxane) (10.5 mL, 42 mmol) was added. The mixture was stirred for 5 h at rt. The reaction mixture was concentrated and purified (silica, EtOAc/MeOH/NEt_3, 200:2:1) to give **7** (0.150 g, 29%) as a white solid. MS-ESI$^+$: *m/z* 247, $[M+H]^+$.

4.1.3.7. (*S*)-1-(*tert*-Butoxycarbonylamino)-N-((1S,2R)-2-hydroxy-1-indanyl)-3-phenylpropanamide (Boc-8). Boc-(*S*)-phenylalanine (669 mg 2.52 mmol), (1*S*,2*R*)-1-amino-2-indanol (458 mg, 3.07 mmol), HOBt (380 mg, 2.81 mmol), EDC (539 mg, 2.81 mmol) were stirred in dry CH_2Cl_2 (50 mL) for 1 h at rt. The reaction mixture was concentrated and purified (silica, 3–5% MeOH in CH_2Cl_2) to give Boc-**8** (1.0 g, quantitative) as a white solid. ^{1}H NMR (400 MHz, CD_3OD): δ = 7.32–7.27 (m, 4H), 7.27–7.15 (m, 5H), 5.29 (d, *J* = 5.1 Hz, 1H), 4.50 (dt, *J* = 5.1, 1.6 Hz, 1H), 4.41 (dd, *J* = 9.7, 5.0 Hz, 1H), 3.25 (dd, *J* = 13.8, 5.0 Hz, 1H), 3.13 (dd, *J* = 16.3, 5.1 Hz, 1H), 2.908 (dd, *J* = 16.3, 1.6 Hz, 1H), 2.907 (dd, *J* = 13.8, 9.7 Hz, 1H), 1.36 ppm (s, 9H); ^{13}C NMR (100 MHz, CD_3OD): δ = 174.7 (2 C=O), 142.2, 141.7, 138.9, 129.4, 128.4, 127.8, 127.7, 126.1, 125.4, 80.7, 73.9, 58.6, 57.7, 40.8, 39.0, 28.6 ppm; MS-ESI$^+$: *m/z* 347, $[M+H]^+$.

4.1.3.8. (*S*)-*N*-((1*S*,2*R*)-2-Hydroxy-1-indanyl)-3-phenylpropanamide (8). Compound Boc-**8** (1.00 g, 2.52 mmol) was dissolved in dioxane (20 mL) and 4 M HCl (1,4-dioxane) (12.5 mL, 50 mmol) was added. The mixture was stirred for 5 h at rt. The volatiles were evaporated in vacuo and the residue was dissolved in DCM and extracted with satd NH_4Cl (aq). The combined aqueous phases were basified to pH 11 with 1 M NaOH (aq) and the product was extracted with EtOAc to give pure **8** (0.273 g, 37%) as a white solid. MS-ESI$^+$: *m/z* 247, $[M+H]^+$.

4.1.4. Experimental details and spectroscopic data for epimeric epoxides (*A*)-9–14 and (*B*)-9–14

4.1.4.1. General procedure for amide coupling reactions. Corresponding carboxylic acid, corresponding amine and PyAOP were suspended in dry CH_2Cl_2, stirred for a few minutes and thereafter diisopropylethylamine was added. The reaction mixture was stirred at rt for 2–5 days. Evaporation afforded the crude products, which were, in the case of **9**,**11**,**13**, and **14**, purified by column chromatography (silica, EtOAc/*i*Hex) prior to the epimeric separation. The epimeric separations of (*R*)-**9**/(*S*)-**9**, (*R*)-**11**/(*S*)-**11**, (*A*)-**13**/(*B*)-**13** and (*A*)-**14**/(*B*)-**14** were performed on a Gilson HPLC system equipped with a chiral (Reprosil Chiral NR-R (8 μm, 250 × 20 mm)) column, using *i*PrOH in *i*Hex as mobile phase at a flow rate of 5 mL/min with UV (230 nm) detection. The epimeric separation was analyzed on a Gilson HPLC system equipped with a chiral (Reprosil Chiral NR-R (8 μm, 250 × 4.6 mm)) column, using *i*PrOH in *i*Hex as mobile phase at a flow rate of 2 mL/min or 1.5 mL/min, as indicated, with UV (220 nm) detection. The epimeric separation of (*R*)- and (*S*)-**10** and (*S*)- and (*R*)-**11** was performed on a Gilson–Finnigan ThermoQuest AQA system C8 (Agilent Zorbax SB-C8 (5 μm, 50 × 21.2 mm)) column, using CH_3CN in 0.05% aqueous HCOOH as mobile phase at a flow rate of 15 mL/min with UV (214 nm) detection and analyzed on a Gilson-Finnigan ThermoQuest AQA system equipped with a C18 (Onyx Monolithic C18 (50 × 4.6 mm)) column, using CH_3CN in 0.05% aqueous HCOOH as mobile phase at a flow rate of 4 mL/min with UV (214 and 254 nm) and MS (ESI$^+$ or ESI$^-$) detection. At room temperature, the NMR spectra of (*S*)-**9**–**12** and (*R*)-**9**–**12** and (*A*)- and (*B*)-**13** indicate the presence of two conformers, due to the cis-trans-isomerism of the thioproline and the proline P1–P1′ amide bond in various ratios (6:1–1:1), which has been confirmed by ^{1}H NMR experiments at a temperature range of 24–60 °C. The shifts at 24 °C of the major conformer are reported, except for (*S*)-**9** and (*R*)-**12**, for which all signals at 24 °C are reported.

4.1.4.2. (4*R*)-*N*-((1*S*,2*R*)-2-Hydroxy-1-indanyl)-5,5-dimethyl-3-(2-phenethyloxirane-2-carbonyl)thiazolidine-4-carboxamide ((*R*)-9 and (*S*)-9). Compound **9** was synthesized according to the general procedure using L-**6** (94.0 mg, 0.321 mmol), **1a** (82.0 mg, 0.427 mmol), PyAOP (240 mg, 0.460 mmol) and DIEA (165 μl, 0.964 mmol). It was purified (silica, EtOAc/*i*Hex, 1:3–3:1) to give **9** (80.0 mg, 53%) as a diastereomeric mixture. The epimers were then separated and further purified by chiral SP-HPLC to give (*R*)-**9** (18.5 mg) and (*S*)-**9** (18.3 mg) as white solids (totally 36.8 mg, 25%). Compound (*S*)-**9**: t_R = 14.3 min (SP-HPLC, 15% *i*PrOH in *i*Hex, 2.0 mL/min); rotamer ratio (5:4); ^{1}H NMR (400 MHz, CD_3OD): ma-

jor conformer: δ = 7.45–7.41 (m, 1H), 7.27–7.13 (m, 8H), 5.38 (dd, J = 5.1, 1.2 Hz, 1H), 5.06 (d, J = 9.8 Hz, 1H), 4.92 (d, J = 9.8 Hz, 1H), 4.52 (dt, J = 5.1, 2.0 Hz, 1H), 4.50 (s, 1H), 3.15 (dd, J = 16.3, 5.1 Hz, 1H), 3.03 (d, J = 4.8 Hz, 1H), 2.932 (dd, J = 16.3, 2.0 Hz, 1H), 2.90 (d, J = 4.8 Hz, 1H), 2.86–2.79 (m, 2H), 2.35–2.27 (m, 1H), 2.15–2.07 (m, 1H), 1.57 (s, 3H), 1.53 ppm (s, 3H); Minor conformer: δ = 7.32–7.27 (m, 1H), 7.27–7.13 (m, 8H), 5.38 (dd, J = 5.1, 1.2 Hz, 1H), 4.91 (d, J = 10.3 Hz, 1H), 4.87 (s, 1H), 4.71 (d, J = 10.3 Hz, 1H), 4.52 (dt, J = 5.1, 2.0 Hz, 1H), 3.14 (dd, J = 16.3, 5.1 Hz, 1H), 2.932 (dd, J = 16.3, 2.0 Hz, 1H), 2.928 (d, J = 5.0 Hz, 1H), 2.92 (d, J = 5.0 Hz, 1H), 2.86–2.79 (m, 1H), 2.70 (ddd, J = 14.2, 11.8, 5.5 Hz, 1H), 2.46 (ddd, J = 14.2, 11.8, 5.4 Hz, 1H), 1.86 (ddd, J = 14.1, 11.7, 5.2 Hz, 1H), 1.58 (s, 3H), 1.54 ppm (s, 3H); ^{13}C NMR (100 MHz, CD_3OD): major conformer: δ = 171.0, 170.1, 142.4, 142.1, 141.60, 129.52, 129.46, 128.90, 127.1, 126.1, 125.9, 74.07, 74.0, 61.0, 58.8, 52.32, 52.1, 50.2, 41.07, 36.0, 31.7, 30.5, 25.1 ppm; minor conformer: δ = 171.6, 171.3, 142.4, 142.3, 141.58, 129.59, 129.3, 128.91, 127.82, 127.3, 126.2, 125.7, 74.10, 72.9, 61.3, 58.5, 52.31, 52.1, 49.5, 41.11, 36.6, 32.2, 31.8, 25.2 ppm; MS-ESI$^+$: m/z 467, [M+H]$^+$. Anal. Calcd for $C_{26}H_{30}N_2O_4S{\cdot}2H_2O$: C, 62.13; H, 6.82; N, 5.57. Found: C, 63.29; H, 5.95; N, 5.45. Compound (*R*)-**9**: t_R = 8.8 min (SP-HPLC, 15% *i*PrOH in *i*Hex, 2.0 mL/min); rotamer ratio (4:1); ^{1}H NMR (400 MHz, CD_3OD) δ = 7.41–7.35 (m, 1H), 7.30–7.11 (m, 8H), 5.36 (d, J = 5.2 Hz, 1H), 4.95 (d, J = 10.4 Hz, 1H), 4.89 (d, J = 10.4 Hz, 1H), 4.53 (s, 1H), 4.50 (dt, J = 5.2, 5.2, 1.0 Hz, 1H), 3.14 (dd, J = 16.3, 5.2 Hz, 1H), 3.04 (d, J = 5.0 Hz, 1H), 2.929 (d, J = 5.0 Hz, 1H), 2.926 (dd, J = 16.3, 2.0 Hz, 1H), 2.87–2.69 (m, 2H), 2.54 (ddd, J = 14.4, 10.6, 5.8 Hz, 1H), 1.91 (ddd, J = 14.4, 10.3, 6.2 Hz, 1H), 1.62 (s, 3H), 1.50 ppm (s, 3H); ^{13}C NMR (100 MHz, CD_3OD) δ = 170.9, 170.3, 142.2, 142.1, 141.6, 129.53, 129.44, 129.0, 127.8, 127.2, 126.1, 125.8, 74.1, 73.9, 60.5, 58.5, 52.3, 52.0, 50.2, 41.0, 35.7, 31.9, 29.0, 25.7 ppm; MS-ESI$^+$: m/z 467, [M+H]$^+$. Anal. Calcd for $C_{26}H_{30}N_2O_4S{\cdot}1/5\ H_2O$: C, 65.42; H, 6.52; N, 5.97. Found: C, 65.86; H, 5.86; N, 5.55.

4.1.4.3. (4*R*)-*N*-((1*S*,2*R*)-2-Hydroxy-1-indanyl)-5,5-dimethyl-3-(2-benzyloxirane-2-carbonyl)thiazolidine-4-carboxamide ((*R*)-10 and (S)-10).

Compound **10** was synthesized according to the general procedure using L-**6** (96.8 mg, 0.33 mmol), **1b** (68.2 + 50.0 mg, 0.383 + 0.280 mmol), PyAOP (202.0 + 101.0 mg, 0.388 + 0.194 mmol), DIEA (180 µl, 1.05 mmol) and 1 mL DMF as co-solvent. The epimers were then separated and purified by RP-HPLC to give (*R*)-**10** (33.3 mg) and (*S*)-**10** (23.4 mg) as white solids (totally 56.7 mg, 38%). Compound (*S*)-**10**: t_R = 1.79 min (RP-HPLC, 10–90%, 4.2 min); t_R = 7.90 min (SP-HPLC, 15% *i*PrOH in *i*Hex, 2.0 mL/min); rotamer ratio (7:4); ^{1}H NMR (400 MHz, CD_3OD): δ = 7.39–7.16 (m, 9H), 5.37 (d, J = 5.0 Hz, 1H), 4.83 (d, J = 10.3 Hz, 1H), 4.50 (dt, J = 5.0, 1.8 Hz, 1H), 4.22 (s, 1H), 4.07 (d, J = 10.3 Hz, 1H), 3.71 (d, J = 14.2 Hz, 1H), 3.14 (dd, J = 16.4, 5.0 Hz, 1H), 3.00 (d, J = 5.2 Hz, 1H), 2.97 (d, J = 5.2 Hz, 1H), 2.93 (dd, J = 16.4, 1.8 Hz, 1H), 2.58 (d, J = 14.2 Hz, 1H), 1.39 (s, 3H), 0.82 ppm (s, 3H); ^{13}C NMR (100 MHz, CD_3OD): δ = 171.7, 170.8, 142.2, 141.5, 137.4, 130.9, 129.9, 129.0, 128.5, 127.8, 126.2, 125.5, 74.1, 73.1, 62.6, 58.3, 52.2, 50.1, 42.2, 41.2, 40.7, 30.7, 24.4 ppm; MS-ESI$^+$: m/z 453, [M+H]$^+$; HRMS-ESI$^+$: m/z [M+H]$^+$ calcd for $C_{25}H_{29}N_2O_4S$: 453.1848, found 453.1844. Compound (*R*)-**10**: t_R = 1.86 min (RP-HPLC, 10–90%, 4.2 min); t_R = 7.88 min (SP-HPLC, 15% *i*PrOH in *i*Hex, 2.0 mL/min); rotamer ratio (10:1); ^{1}H NMR (400 MHz, CD_3OD:$CDCl_3$): δ = 7.36–7.14 (m, 9H), 5.33 (dd, J = 5.2, 1.1 Hz, 1H), 4.79 (d, J = 10.2 Hz, 1H), 4.48 (dt, J = 5.2, 1.9 Hz, 1H), 4.39 (s, 1H), 4.04 (d, J = 10.2 Hz, 1H), 3.65 (d, J = 14.2 Hz, 1H), 3.13 (dd, J = 16.4, 5.2 Hz, 1H), 3.09 (d, J = 5.1 Hz, 1H), 2.94 (d, J = 5.1 Hz, 1H), 2.91 (dd, J = 16.4, 1.9 Hz, 1H), 2.68 (d, J = 14.2 Hz, 1H), 1.41 (s, 3H), 1.40 ppm (s, 3H); ^{13}C NMR (100 MHz, CD_3OD:$CDCl_3$): δ = 170.8, 170.2, 142.0, 141.4, 136.8, 130.6, 129.7, 128.9, 128.4, 127.8, 126.0, 125.6, 74.1, 73.8, 61.9, 58.3, 52.6, 51.5, 49.5, 41.0, 40.3, 29.0, 25.3 ppm; MS-ESI$^+$: m/z 453, [M+H]$^+$; HRMS-ESI$^+$: m/z [M+H]$^+$ calcd for $C_{25}H_{29}N_2O_4S$: 453.1848, found 453.1855.

4.1.4.4. (4*S*)-*N*-((1*S*,2*R*)-2-Hydroxy-1-indanyl)-5,5-dimethyl-3-(2-phenethyloxirane-2-carbonyl)thiazolidine-4-carboxamide ((*S*)-11 and (*R*)-11).

Compound **11** was synthesized according to the general procedure using D-**6** (94.0 mg, 0.322 mmol), **1a** (92.0 mg, 0.427 mmol), PyAOP (324 mg, 0.621 mmol) and DIEA (182 µl, 1.06 mmol). It was purified (silica, EtOAc/iHex, 1:3–3:1) to give **11** as a diastereomeric mixture. The epimers were then separated and further purified by chiral HPLC to give (*S*)-**11** (57.6 mg) and (*R*)-**11** (39.8 mg) as white solids (totally 36.8 mg, 65%). Compound (*S*)-**11**: t_R = 9.4 min (SP-HPLC, 15% *i*PrOH in *i*Hex, 1.5 mL/min); rotamer ratio (3:1); ^{1}H NMR (400 MHz, CD_3OD): δ = 7.29–7.13 (m, 9H), 5.30 (d, J = 5.0 Hz, 1H), 4.96 (d, J = 10.3 Hz, 1H), 4.90 (d, J = 10.3 Hz, 1H), 4.59 (dt, J = 5.0, 1.6 Hz, 1H), 4.49 (s, 1H), 3.14 (dd, J = 16.5, 5.1 Hz, 1H), 2.97–2.95 (m, 1H), 2.91 (d, J = 5.0 Hz, 1H), 2.89 (d, J = 5.0 Hz, 1H), 2.84–2.67 (m, 3H), 2.52–2.43 (m, 1H), 1.96–1.86 (m, 1H), 1.62 (s, 3H), 1.52 ppm (s, 3H); ^{13}C NMR (100 MHz, CD_3OD): δ = 170.9, 170.7, 142.0, 141.9, 141.8, 129.51, 129.45, 129.1, 127.8, 127.2, 126.2, 125.3, 74.2, 73.9, 60.5, 59.1, 52.3 51.9 50.1, 40.6, 35.6, 31.9, 29.2, 25.6 ppm; MS-ESI$^+$: m/z 467, [M+H]$^+$. Anal. Calcd for $C_{26}H_{30}N_2O_4S{\cdot}1/3H_2O$: C, 66.08; H, 6.54; N, 5.93. Found: C, 66.28; H, 6.55; N, 5.82. Compound (*R*)-**11**: t_R = 11.8 min (SP-HPLC, 15% *i*PrOH in *i*Hex, 1.5 mL/min); rotamer ratio (3:1); ^{1}H NMR (CD_3OD) δ = 7.32–7.08 (m, 9H), 5.33 (d, J = 5.0 Hz, 1H), 5.03 (d, J = 10.0 Hz, 1H), 4.93 (d, J = 10.0 Hz, 1H), 4.62 (dt, J = 5.0, 1.5 Hz, 1H), 4.44 (s, 1H), 3.14 (dd, J = 16.4, 5.0 Hz, 1H), 2.96 (d, J = 4.8 Hz, 1H), 2.94 (dd, J = 16.4, 1.5 Hz, 1H), 2.87 (d, J = 4.8 Hz, 1H), 2.29–2.20 (m, 1H), 2.06–1.98 (m, 1H), 1.57 (s, 3H), 1.54 ppm (s, 3H); ^{13}C NMR (100 MHz, CD_3OD): δ = 171.5, 170.1, 142.2, 141.94, 141.87, 129.58, 129.38, 129.0, 127.8, 127.1, 126.2, 125.4, 74.3, 73.8, 61.0, 59.2, 52.24 51.9 50.2, 40.6, 36.1, 31.8, 30.5, 24.8 ppm; MS-ESI$^+$: m/z 467, [M+H]$^+$. Anal. Calcd for $C_{26}H_{30}N_2O_4S{\cdot}1/2H_2O$: C, 65.66; H, 6.57; N, 5.89. Found: C, 65.57; H, 6.58; N, 5.89.

4.1.4.5. (4*S*)-*N*-((1*S*,2*R*)-2-Hydroxy-1-indanyl)-5,5-dimethyl-3-(2-benzyloxirane-2-carbonyl)thiazolidine-4-carboxamide ((*S*)-12 and (*R*)-12).

Compound **12** was synthesized according to the general procedure using D-**6** (93.8 mg, 0.320 mmol), **1b** (142 mg, 0.798 mmol), PyAOP (415 mg, 0.796 mmol), DIEA (250 µl, 1.46 mmol) and 1 mL DMF as co-solvent. The epimers were then separated and purified by RP-HPLC to give pure (*S*)-**12** (36.2 mg) and (*R*)-**12** (24.8 mg) and mixed epimers as white solids (totally 82.8 mg, 57%). Compound (*S*)-**12**: t_R = 2.09 min (RP-HPLC, 10–90%, 4.2 min); t_R = 6.90 min (SP-HPLC, 15% *i*PrOH in *i*Hex, 2.0 mL/min); rotamer ratio (6:1), ^{1}H NMR (400 MHz, CD_3OD): δ = 7.34–7.16 (m, 9H), 5.28 (d, J = 5.0 Hz, 1H), 4.80 (d, J = 10.2 Hz, 1H), 4.56 (dt, J = 5.0, 1.6 Hz, 1H), 4.38 (s, 1H), 4.07 (d, J = 10.2, 1H), 3.63 (d, J = 14.2, 1H), 3.14 (ddd, J = 16.4, 5.0, 1.1 Hz, 1H), 2.932 (d, J = 5.05 Hz, 1H), 2.926 (ddd, J = 16.4, 1.6, 0.5 Hz, 1H), 2.91 (d, J = 5.05 Hz, 1H), 2.69 (d, J = 14.2 Hz, 1H), 1.42 (s, 3H), 1.41 ppm (s, 3H); ^{13}C NMR (100 MHz, CD_3OD): δ = 170.9, 170.7, 141.9, 141.8, 137.0, 130.7, 129.8, 129.1, 128.5, 127.8, 126.3, 125.2, 74.2, 73.9, 62.1, 59.0, 52.6, 51.6, 49.3, 40.6, 40.3, 29.1, 25.3 ppm; MS-ESI$^+$: m/z 453, [M+H]$^+$; HRMS-ESI$^+$: m/z [M+H]$^+$ calcd for $C_{25}H_{29}N_2O_4S$: 453.1848, found 453.1859. Compound (*R*)-**12**: t_R = 2.16 min (RP-HPLC, 10–90%, 4.2 min); t_R = 6.92 min (SP-HPLC, 15% *i*PrOH in *i*Hex, 2.0 mL/min); rotamer ratio (1:1), the lower shift in brackets; ^{1}H NMR (400 MHz, CD_3OD): δ = 7.35–7.18 (m, 9+9H), 5.37 (d, J = 5.0 Hz, 1H) (5.25 (d, J = 5.2 Hz, 1H)), 4.80 (d, J = 9.8 Hz, 1H) (4.63 (d, J = 10.6 Hz, 1H)), 4.61 (dt, J = 5.0, 1.5 Hz, 1H) (4.56 (dt, J = 5.2, 2.1 Hz, 1H)), 4.44 (d, J = 9.8 Hz, 1H) 4.58 (d, J = 10.6 Hz, 1H), 4.35 (s, 1H) (4.23 (s, 1H)), 3.61 (d, J = 14.2, 1H) (3.05 (d, J = 14.3, 1H)), 3.30 (d, J = 14.2, 1H) (2.61 (d, J = 14.3,

1H)), 3.20–3.12 (m, 2H), 3.00 (d, *J* = 4.9 Hz, 1H) (2.92 (d, *J* = 4.9 Hz, 1H)), 2.96 (dd, *J* = 16.4, 1.5 Hz, 1H) (2.94 (dd, *J* = 16.4, 2.1 Hz, 1H)), 2.69 (d, *J* = 4.9 Hz, 1H) (2.84 (d, *J* = 4.9 Hz, 1H)), 1.52 (s, 3 H), 1.49 (s, 3H), 1.38 (s, 3H), 0.84 ppm (s, 3H); ^{13}C NMR (100 MHz, CD_3OD): δ = 172.0 (171.7), 171.0 (170.0), 142.04 (141.99), 141.9, 137.2 (136.0), 131.1 (130.9), 129.9 (129.7), 129.13 (129.06), 128.5 (128.3), 127.83 (127.81), 126.2, 125.9 (125.4), 74.3 (73.9), 73.8 (72.9), 63.1 (61.5), 59.2 (58.9), 54.7 (52.9), 52.45 (52.42), 50.1 (49.5), 40.63 (40.61), 40.54 (39.5), 30.7 (30.3), 25.0 (24.8) ppm; MS-ESI$^+$: *m/z* 453, $[M+H]^+$; HRMS-ESI$^+$: $[M+H]^+$ calcd for $C_{25}H_{29}N_2O_4S$: 453.1848, found 453.1841.

4.1.4.6. (5*S*)-*N*-((1*S*,2*R*)-2-Hydroxy-1-indanyl)-1-(2-phenethyloxirane-2-carbonyl)pyrrolidine-5-carboxamide ((*A*)-13 and (*B*)-13). Compound **13** was synthesized according to the general procedure using L-**7** (70.0 mg, 0.284 mmol), **1a** (60.01 mg, 0.3126 mmol), PyAOP (240 mg, 0.460 mmol) and DIEA (160 µl, 0.94 mmol). It was purified (silica, EtOAc/MeOH, 99:1–98:2) to give **13** as a diastereomeric mixture. The epimers were then separated and further purified by chiral HPLC to give (*A*)-**13** (36.6 mg) and (*B*)-**13** (37.3 mg) as white solids (totally 73.9 mg, 62%). Compound (*A*)-**13**: t_R = 12.5 min (SP-HPLC, 15% *i*PrOH in *i*Hex, 1.5 mL/min); rotamer ratio (4:1), ^{1}H NMR (400 MHz, CD_3OD): δ = 7.40–7.33 (m, 1H), 7.29–7.11(m, 9H), 5.31 (d, *J* = 5.0 Hz, 1H), 4.55–4.48 (m, 2H), 3.80–3.68 (m, 2H), 3.14 (dd, *J* = 16.4, 5.1 Hz, 1H), 2.98 (d, *J* = 5.1 Hz, 1H), 2.91 (d, *J* = 5.0 Hz, 1H), 2.96–2.87 (m, 1H), 2.83–2.70 (m, 2H), 2.28–2.13 (m, 1H), 2.12–1.94 (m, 2H), 1.94–1.81 ppm (m, 2H); ^{13}C NMR (100 MHz, CD_3OD): δ = 174.2, 170.9, 142.3, 142.1, 141.5, 129.47, 129.44, 128.9, 127.9, 127.1, 126.1, 125.6, 74.0, 62.1, 60.5, 58.7, 52.2, 49.1, 40.8, 35.6, 31.8, 30.2, 26.4 ppm; MS-ESI$^+$: *m/z* 421, $[M+H]^+$. Anal. Calcd for $C_{25}H_{28}N_2O_4 \cdot 1/2\ H_2O$: C, 69.91; H, 6.81; N, 6.52. Found: C, 69.89; H, 6.83; N, 6.19. Compound (*B*)-**13**: t_R = 17.5 min (SP-HPLC, 15% *i*PrOH in *i*Hex, 1.5 mL/min); rotamer ratio (4:3), ^{1}H NMR (400 MHz, CD_3OD): δ = 7.42–7.39 (m, 1H), 7.29–7.13 (m, 8H), 5.33 (dd, *J* = 5.1, 1.0 Hz, 1H), 4.81 (dd, *J* = 8.2, 1.3 Hz, 1H), 4.51 (dt, *J* = 5.1, 2.0 Hz, 1H), 3.89–3.76 (m, 2H), 3.15 (dd, *J* = 16.4, 5.1 Hz, 1H), 2.98 (d, *J* = 4.9 Hz, 1H), 2.93 (d, *J* = 16.4 Hz, 1H), 2.88 (d, *J* = 4.9 Hz, 1H), 2.85–2.79 (m, 1H), 2.79–2.63 (m, 1H), 2.24–2.00 (m, 5H), 1.89–1.82 ppm (m, 1H); ^{13}C NMR (100 MHz, CD_3OD): δ = 174.5, 170.1, 142.44, 142.38, 141.6, 129.5, 129.4, 128.9, 127.9, 127.1, 126.0, 125.8, 74.0, 61.0, 58.8, 52.2, 48.6, 40.8, 36.1, 31.8, 30.3, 26.0 ppm; MS-ESI$^+$: *m/z* 421, $[M+H]^+$. Anal. Calcd for $C_{25}H_{28}N_2O_4 \cdot H_2O$: C, 68.47; H, 6.90; N, 6.39. Found: C, 68.75; H, 6.90; N, 6.09.

4.1.4.7. (2*S*)-*N*-((1*S*,2*R*)-2-Hydroxy-1-indanyl)-2-(2-phenethyloxirane-2-carbonyl)amino-3-phenylpropylamide ((*A*)-14 and (*B*)-14). Compound **14** was synthesized according to the general procedure using **8** (94.5 mg, 0.32 mmol), **1a** (67.4 + 20.0 mg, 0.35 + 0.10 mmol), PyBOP (199 + 68 mg, 0.383 + 0.13 mmol) and DIEA (180 µl, 1.05 mmol). It was purified (silica, EtOAc/iHex, 1:3–3:1) to give **14** as a diastereomeric mixture. The epimers were then separated and purified by chiral HPLC to give (*A*)-**14** (23.4 mg) and (*B*)-**14** (21.7 mg) as white solids (totally 45.1 mg, 30%). Compound (*A*)-**14**: t_R = 12.08 min (SP-HPLC, 20% *i*PrOH in *i*Hex, 2.0 mL/min); ^{1}H NMR (400 MHz, CD_3OD): δ = 7.34–7.11 (m, 12H), 7.06–7.03 (m, 2H), 5.29 (d, *J* = 5.2 Hz, 1H), 4.81 (dd, *J* = 10.3, 4.8 Hz, 1H), 4.52 (dt, *J* = 5.2, 2.0 Hz, 1H), 3.32 (dd, *J* = 14.0, 4.8 Hz, 1H), 3.15 (ddd, *J* = 16.4, 5.2, 1.0 Hz, 1H), 2.99 (dd, *J* = 14.0, 10.4 Hz, 1H), 2.92 (dd, *J* = 16.4, 2.0 Hz, 1H), 2.84 (s, 2H), 2.50–2.40 (m, 1H), 2.29–2.19 (m, 1H), 1.54–1.47 ppm (m, 1H); ^{13}C NMR (100 MHz, CD_3OD): δ = 173.6, 172.4, 142.5, 142.2, 141.7, 138.5, 130.5, 129.6, 129.4, 129.3, 129.0, 127.90, 127.86, 127.0, 126.2, 125.4, 73.8, 59.9, 58.6, 55.7, 53.8, 40.8, 38.8, 34.4, 31.8 ppm; MS-ESI$^+$: *m/z* 471, $[M+H]^+$; HRMS-ESI$^+$: $[M+H]^+$ calcd for $C_{29}H_{31}N_2O_4$: 471.2284, found: 471.2287. Compound (*B*)-**14**: t_R = 16.63 min (SP-HPLC, 20% *i*PrOH in *i*Hex, 2.0 mL/min); ^{1}H NMR (400 MHz, CD_3OD): δ = 7.31–7.09 (m, 14H), 5.31 (d, *J* = 5.1 Hz, 1H), 4.77 (dd, *J* = 10.1, 5.0 Hz, 1H), 4.54 (dt, *J* = 5.0, 2.1 Hz, 1H), 3.29 (dd, *J* = 13.9, 5.0 Hz, 1H), 3.14 (dd, *J* = 16.4, 5.2 Hz, 1H), 2.98 (dd, *J* = 13.9, 10.1 Hz, 1H), 2.92 (dd, *J* = 16.4, 2.1 Hz, 1H), 2.72 (d, *J* = 5.2 Hz, 1H), 2.67–2.61 (m, 2H), 2.50–2.42 (m, 1H), 2.27 (d, *J* = 5.2 Hz, 1H), 1.54–1.47 ppm (m, 1H); ^{13}C NMR (100 MHz, CD_3OD): δ = 173.5, 172.6, 142.5, 142.2, 141.8, 138.5, 130.4, 129.5, 129.38, 129.37, 129.0, 127.89, 127.85, 127.0, 126.2, 125.4, 73.8, 59.7, 58.7, 55.3, 53.6, 40.8, 38.6, 34.3, 31.9 ppm; MS-ESI$^+$: *m/z* 471, $[M+H]^+$; HRMS-ESI$^+$: $[M+H]^+$ calcd for $C_{29}H_{31}N_2O_4$: 471.2284, found: 471.2289.

4.1.5. Experimental details and spectroscopic data for inhibitors (*S*)-15–18, (*R*)-15–18, (*A*)-19,20 and (*B*)-19,20

4.1.5.1. General procedure for epoxide ring opening reactions. Epoxide, 500 equiv of aqueous NH_3 (25%) and the equivalent volume of methanol was stirred in room temperature overnight. The volatiles were evaporated in vacuo and the residue was used in the proceeding amide coupling without any further purification.

4.1.5.2. General procedure for amide coupling reactions. Carboxylic acid, amine and PyBOP were dissolved in dry CH_2Cl_2, stirred for a few minutes and thereafter Hünig's base (DIEA) was added. The reaction mixture was stirred at room temp for 24 h. Evaporation afforded the crude product, which was purified on RP-HPLC and freeze-dried to give the final products. At room temperature, the NMR spectra of (*S*)-**15**–**17**, (*R*)-**17**, (*B*)-**18** and (*A*)-**19** indicate the presence of two conformers, due to the cis-trans-isomerism of the thioproline and the proline P1–P1′ amide bond in various ratios (>10:1–9:8), which has been confirmed by ^{1}H NMR experiments at a temperature range of 24–60 °C. The shifts at 24 °C of the major conformer are reported, except for (*S*)-**16** and (*B*)-**18** for which all signals are reported.

4.1.5.3. (*S*)-(4*S*)-*N*-((1S,2R)-2-Hydroxy-1-indanyl)-3-(2-phenethyl-3-(2-(2,6-dimethylphenoxy)acetamido)-2-hydroxypropanoyl)-5,5-dimethylthiazolidine-4-carboxamide ((*S*)-15). Compound (*S*)-**15** was synthesized according to the general procedure from (*S*)-**9** (14.5 mg, 0.030 mmol), **21** (7.1 mg, 0.039 mmol), PyBOP (28.6 mg, 0.055 mmol) and DIEA (12.0 µl, 0.070 mmol). 0.30 mL of DMF was added as co-solvent. It was purified (RP-HPLC) to give (*S*)-**15** as a white solid (9.83 mg, 51%). Compound (*S*)-**15**: t_R = 17.83 (SP-HPLC, 15% *i*PrOH in *i*Hex); $[\alpha]_D^{21}$ = +5.5 (*c* 0.181, MeOH); rotamer ratio (3:1); ^{1}H NMR (400 MHz, CD_3OD): δ = 7.40–7.37 (m, 1H), 7.29–7.10 (m, 8H), 7.04–6.97 (m, 2H), 6.92 (dd, *J* = 8.4, 6.4 Hz, 1 H), 5.47 (d, *J* = 10.4 Hz, 1H), 5.33 (d, *J* = 5.0 Hz, 1H), 5.17 (d, *J* = 10.4 Hz, 1H), 4.59 (s, 1H), 4.50 (dt, *J* = 5.0, 1.8 Hz, 1H), 4.23 (s, 2H), 3.87 (d, *J* = 13.7 Hz, 1H), 3.63 (d, *J* = 13.7 Hz, 1H), 2.88 (dd, *J* = 16.3, 5.0 Hz, 1H), 2.85–2.72 (m, 2H), 2.27 (ddd, *J* = 13.8, 12.6, 4.7 Hz, 1H), 2.24 (s, 6H), 2.00 (ddd, *J* = 13.8, 12.6, 5.6 Hz, 1H), 1.63 (s, 3H), 1.53 ppm (s, 3H); ^{13}C NMR (100 MHz, CD_3OD): δ = 174.5, 171.9, 171.4, 156.0, 143.5, 142.3, 141.5, 131.8, 130.0, 129.5, 129.4, 128.8, 127.8, 126.9, 125.97, 125.95, 125.8, 80.1, 75.8, 74.1, 71.3, 58.9, 50.9, 50.6, 47.1, 40.9, 39.8, 30.8, 29.8, 25.5, 16.5 ppm; MS-ESI$^+$: *m/z* 646, $[M+H]^+$; HRMS-ESI$^+$: $[M+H]^+$ calcd for $C_{36}H_{44}N_3O_6S$: 646.2951, found: 646.2963. Anal. Calcd for $C_{36}H_{43}N_3O_6S \cdot 2/5\ H_2O$: C, 66.21; H, 6.76; N, 6.43. Found: C, 65.89; H, 6.36; N, 6.09.

4.1.5.4. (*R*)-(4*S*)-*N*-((1S,2R)-2-Hydroxy-1-indanyl)-3-(2-phenethyl-3-(2-(2,6-dimethylphenoxy)acetamido)-2-hydroxypropanoyl)-5,5-dimethylthiazolidine-4-carboxamide ((*R*)-15). Compound (*R*)-**15** was synthesized according to the general procedure from (*R*)-**9** (14.5 mg, 0.030 mmol), **21** (7.1 mg, 0.039 mmol), PyBOP (28.6 mg, 0.055 mmol) and DIEA (12.0 µl, 0.070 mmol). It was purified (RP-HPLC) to give (*R*)-**15** as a white solid (10.3 mg, 53%). Compound (*R*)-

15: t_R = 21.12 (SP-HPLC, 15% *i*PrOH in *i*Hex); $[\alpha]_D^{21}$ = −1.5 (*c* 0.027, MeOH); rotamer ratio (>10:1); ^{1}H NMR (400 MHz, CD_3OD): δ = 7.35 (d, *J* = 7.5 Hz, 1H), 7.290–6.86 (m, 11H), 5.39 (d, *J* = 10.8 Hz, 1H), 5.29 (d, *J* = 5.0 Hz, 1H), 5.17 (d, *J* = 10.8 Hz, 1H), 4.54 (s, 1H), 4.48 (dt, *J* = 5.0, 1.8 Hz, 1H), 4.26 (d, 14.8 Hz, 1H), 4.14 (d, *J* = 14.8 Hz, 1H), 3.79 (d, *J* = 13.7 Hz, 1H), 3.75 (d, *J* = 13.7 Hz, 1H), 3.02 (dd, *J* = 16.4, 5.0 Hz, 1H), 2.84 (dd, *J* = 16.4, 1.8 Hz, 1H), 2.83–2.66 (m, 2H), 2.23–2.14 (m, 1H), 2.21 (s, 6H), 2.03–1.94 (m, 1H), 1.62 (s, 3H), 1.52 ppm (s, 3H); ^{13}C NMR (100 MHz, CD_3OD): δ = 174.7, 172.0, 171.3, 156.0, 143.2, 141.9, 141.6, 131.8, 130.0, 129.5, 129.4, 128.8, 127.7, 127.0, 126.0, 125.8, 125.7, 79.8, 75.8, 74.0, 71.2, 58.9, 50.9, 50.7, 47.1, 40.9, 39.7, 30.9, 29.1, 25.7, 16.5 ppm; MS-ESI$^+$: *m*/*z* 646, $[M+H]^+$; HRMS-ESI$^+$: $[M+H]^+$ calcd for $C_{36}H_{44}N_3O_6S$: 646.2951, found 646.2955. Anal. Calcd for $C_{36}H_{43}N_3O_6S$: C, 66.95; H, 6.71; N, 6.51. Found: C, 65.71; H, 6.83; N, 6.33.

4.1.5.5. (*S*)-(4*S*)-3-(2-Benzyl-3-(2-(2,6-dimethylphenoxy)acetamido)-2-hydroxypropanoyl)-*N*-((1*S*,2*R*)-2-hydroxy-1-indanyl)-5,5-dimethylthiazolidine-4-carboxamide ((*S*)-16). Compound (*S*)-**16** was synthesized according to the general procedure from (*S*)-**10** (24.0 mg, 0.053 mmol), **21** (12.8 mg, 0.071 mmol), PyBOP (46.4 mg, 0.089 mmol) and DIEA (30.0 μl, 0.175 mmol). It was purified (RP-HPLC) to give (*S*)-**16** as a white solid (20.9 mg, 62%). Compound (*S*)-**16**: t_R = 15.72 (SP-HPLC, 15% *i*PrOH in *i*Hex); $[\alpha]_D^{22}$ = −23.4 (*c* 0.82, MeOH); rotamer ratio (9:8); ^{1}H NMR (400 MHz, CD_3OD): δ = 7.37–7.33 (m, 2+2H), 7.29–7.07 (m, 7+7H), 7.05–6.88 (m, 3+3H), 5.35 (d, *J* = 10.4 Hz, 1H) (4.75 (d, *J* = 10.9 Hz, 1H)), 5.33 (d, *J* = 4.9 Hz, 1H) (5.32 (d, *J* = 4.9 Hz, 1H)), 4.79 (d, *J* = 10.4 Hz, 1H) (4.53 (d, *J* = 10.9 Hz, 1H)), 4.54 (dt, *J* = 4.9, 1.6 Hz, 1H) (4.46 (dt, *J* = 4.9, 1.8 Hz, 1H)), 4.52 (s, 1H) (4.31 (s, 1H)), 4.41 (s, 2H) (4.17 (d, *J* = 14.8 Hz, 1H), 4.12 (d, *J* = 14.8 Hz, 1H)), 3.95(d, *J* = 13.7 Hz, 1H) (3.85 (d, *J* = 13.7 Hz, 1H)), 3.52 (d, *J* = 13.7 Hz, 1H) (3.70 (d, *J* = 13.7 Hz, 1H)), 3.23 (d, *J* = 13.6 Hz, 1H) (3.20 (d, *J* = 13.1 Hz, 1H)), 3.12 (d, *J* = 14.0 Hz, 1H) (2.92 (d, *J* = 13.4 Hz, 1H)), 3.11 (dd, *J* = 16.6, 4.9 Hz, 1H) (2.98 (dd, *J* = 16.3, 4.9 Hz, 1H)), 2.85 (dd, *J* = 16.3, 2.0 Hz, 1+1H), 2.24 (s, 6H) (2.23 (s, 6H)), 1.57 (s, 3H) (1.51 (s, 3H)), 1.37 ppm (s, 3H) (0.84 ppm (s, 3H)); ^{13}C NMR (100 MHz, CD_3OD): major rotamer: δ = 174.4, 172.9, 172.1, 156.0, 141.98, 141.73, 137.3, 132.0, 131.71, 130.07, 129.2, 128.9, 128.1, 127.78, 126.12, 125.8, 125.66, 82.5, 76.1, 74.0, 71.28, 59.1, 51.0, 50.5, 47.2, 43.7, 41.0, 29.9, 25.4, 16.6 ppm; minor rotamer: δ = 175.2, 173.1, 171.4, 156.0, 142.06, 141.7, 136.7, 131.9, 130.72, 130.05, 129.5, 129.5, 127.9, 127.83, 126.07, 125.9, 125.74, 80.3, 74.1, 74.5, 71.33, 58.7, 51.70, 50.5, 45.4, 43.7, 40.8, 30.9, 25.4, 16.4 ppm; MS-ESI$^+$: *m*/*z* 632, $[M+H]^+$; HRMS-ESI$^-$: $[M-H]^+$ calcd for $C_{35}H_{40}N_3O_6S$: 630.2638, found 630.2647.

4.1.5.6. (*R*)-(4*S*)-3-(2-Benzyl-3-(2-(2,6-dimethylphenoxy)acetamido)-2-hydroxypropanoyl)-*N*-((1*S*,2*R*)-2-hydroxy-1-indanyl)-5,5-dimethylthiazolidine-4-carboxamide ((*R*)-16). Compound (*R*)-**16** was synthesized according to the general procedure from (*R*)-**10** (18.7 mg, 0.040 mmol), **21** (8.6 mg, 0.048 mmol), PyBOP (35.1 mg, 0.067 mmol) and DIEA (15.0 μl, 0.088 mmol). It was purified (RP-HPLC) to give (*R*)-**16** as a white solid (8.11 mg, 37%). Compound (*R*)-**16**: t_R = 19.40 (SP-HPLC, 15% *i*PrOH in *i*Hex); $[\alpha]_D^{21}$ = −47.5 (*c* 0.356, MeOH); ^{1}H NMR (400 MHz, CD_3OD): δ = 7.37–7.21 (m, 6H), 7.17–7.08 (m, 2H), 7.03 (d, *J* = 7.2 Hz, 1H), 6.95 (d, *J* = 7.5 Hz, 2H), 6.90 (dd, *J* = 8.5, 6.2 Hz, 1H), 5.28 (d, *J* = 5.1 Hz, 1H), 4.84 (d, *J* = 10.8 Hz, 1H), 4.47 (dt, *J* = 5.1, 1.7 Hz, 1H), 4.40 (s, 1H), 4.33 (d, *J* = 14.8 Hz, 1H), 4.26 (d, *J* = 14.8 Hz, 1H), 4.2 (d, *J* = 10.8 Hz, 1H), 3.76 (s, 2H), 3.19 (d, *J* = 13.5 Hz, 1H), 3.04 (dd, *J* = 16.4, 5.0 Hz, 1H), 2.95 (d, *J* = 13.5 Hz, 1H), 2.86 (ddd, *J* = 16.4, 1.7, 0.6 Hz, 1H), 2.25 (s, 6H), 1.45 (s, 3H), 1.39 ppm (s, 3H); ^{13}C NMR (100 MHz, CD_3OD): δ = 174.9, 172.1, 171.2, 156.1, 142.0, 141.5, 137.2, 131.8, 131.5, 130.1, 129.5, 128.8, 128.1, 127.8, 126.0, 125.70, 125.69, 81.1, 75.9, 74.1, 71.3, 58.7, 50.45, 50.44, 48.9, 44.2, 41.0, 28.7, 25.6, 16.5 ppm; MS-ESI$^+$: *m*/*z* 632, $[M+H]^+$; HRMS-ESI$^-$: $[M-H]^+$ calcd for $C_{35}H_{40}N_3O_6S$: 630.2638, found 630.2640.

4.1.5.7. (*S*)-(4*S*)-*N*-((1*S*,2*R*)-2-Hydroxy-1-indanyl)-3-(2-phenethyl-3-(2-(2,6-dimethylphenoxy)acetamido)-2-hydroxypropanoyl)-5,5-dimethylthiazolidine-4-carboxamide ((*S*)-17). Compound (*S*)-**17** was synthesized according to the general procedure from (*S*)-**11** (37.9 mg, 0.081 mmol), **21** (17.6 mg, 0.098 mmol), PyBOP (63.4 mg, 0.12 mmol) and DIEA (30.6 μl, 0.18 mmol). It was purified (RP-HPLC) to give (*S*)-**17** as a white solid (28.7 mg, 55%). Compound (*S*)-**17**: t_R = 16.52 (SP-HPLC, 15% *i*PrOH in *i*Hex); $[\alpha]_D^{22}$ = +4.4 (*c* 0.313, MeOH); rotamer ratio (>10:1); ^{1}H NMR (400 MHz, CD_3OD): δ= 7.28–7.13 (m, 9H), 7.04–7.00 (m, 2H), 6.95 (dd, *J* = 8.4, 6.4 Hz, 1H), 5.35 (d, *J* = 10.8 Hz, 1H), 5.22 (d, *J* = 10.8 Hz, 1H), 5.22 (dd, *J* = 4.9, 1.0 Hz, 1H), 4.53 (s, 1H), 4.46 (dt, *J* = 4.9, 1.7 Hz, 1H), 4.30 (d, *J* = 14.8 Hz, 1H), 4.23 (d, *J* = 14.8 Hz, 1H), 3.78 (d, *J* = 13.8 Hz, 1H), 3.73 (d, *J* = 13.8 Hz, 1H), 2.82 (dd, *J* = 16.5, 4.9 Hz, 1H), 2.74 (dd, *J* = 16.5, 1.7 Hz, 1H), 2.79–2.64 (m, 2H), 2.27 (s, 6H), 2.19 (ddd, *J* = 13.9, 12.1, 5.1 Hz, 1H), 1.97 (ddd, *J* = 13.9, 12.1, 5.2 Hz, 1H), 1.63 (s, 3H), 1.54 ppm (s, 3H); ^{13}C NMR (100 MHz, CD_3OD): δ = 174.5, 171.8, 170.0, 155.9, 143.0, 142.0, 141.7, 131.9, 130.1, 129.5, 129.4, 129.0, 127.7, 127.0, 126.2, 125.8, 125.2, 80.1, 75.7, 73.9, 71.2, 59.5, 50.9, 50.7, 47.2, 40.1, 39.7, 30.9, 29.4, 25.6, 16.5 ppm; MS-ESI$^+$: *m*/*z* 646, $[M+H]^+$; HRMS-ESI$^+$: $[M+H]^+$ calcd for $C_{36}H_{44}N_3O_6S$: 646.2951, found 646.2959. Anal. Calcd for $C_{36}H_{43}N_3O_6S{\cdot}2/5\ CHCl_3$: C, 63.04; H, 6.31; N, 6.06. Found: C, 63.45; H, 5.94; N, 5.78 (retrieved from the NMR sample).

4.1.5.8. (*R*)-(4*S*)-*N*-((1*S*,2*R*)-2-Hydroxy-1-indanyl)-3-(2-(2,6-dimethylphenoxyacetyl)amino-2-hydroxy-4-phenylbutanoyl)-5,5-dimethyl-1,3-thiazolidine-4-carboxamide ((*R*)-17). Compound (*R*)-**17** was synthesized according to the general procedure from (*R*)-**11** (22.2 mg, 0.048 mmol), **21** (10.3 mg, 0.057 mmol), PyBOP (37.2 mg, 0.071 mmol) and DIEA (24.4 μl, 0.14 mmol). It was purified (RP-HPLC) to give (*R*)-**17** as a white solid (20.6 mg, 67%). Compound (*R*)-**17**: t_R = 22.15 (SP-HPLC, 15% *i*PrOH in *i*Hex); $[\alpha]_D^{21}$ = −1.5 (*c* 0.160, MeOH); rotamer ratio (5:1); ^{1}H NMR (400 MHz, CD_3OD): δ = 7.28–7.06 (m, 9H), 7.04–6.99 (m, 2H), 6.95 (dd, *J* = 8.4, 6.5 Hz, 1H), 5.43 (d, *J* = 10.6 Hz, 1H), 5.27 (dd, *J* = 8.4, 5.0 Hz, 1H), 5.18 (d, *J* = 10.6 Hz, 1H), 4.57 (dt, *J* = 5.0, 1.3 Hz, 1H), 4.53 (s, 1H), 4.28 (s, 2H), 3.81 (dd, *J* = 13.7, 4.5 Hz, 1H), 3.66 (dd, *J* = 13.7, 4.6 Hz, 1H), 3.06 (dd, *J* = 16.5, 5.0 Hz, 1H), 2.85 (d, *J* = 16.5 Hz, 1H), 2.76 (dt, *J* = 12.9, 4.9 Hz, 1H), 2.63 (ddd, *J* = 12.9, 12.9, 4.7 Hz, 1H), 2.25 (s, 6H), 2.16 (ddd, *J* = 13.7, 12.8, 4.7 Hz, 1H), 1.95 (ddd, *J* = 13.7, 12.9, 4.9 Hz, 1H), 1.63 (s, 3H), 1.55 ppm (s, 3H); ^{13}C NMR (100 MHz, CD_3OD): δ = 174.6, 172.0, 171.0, 155.9, 143.3, 142.0, 141.7, 131.7, 130.1, 129. 5, 129.4, 129.0, 127.8, 126.8, 126.1, 125.8, 125.4, 80.3, 76.0, 73.8, 71.3, 59.4, 50.7, 50.6, 47.2, 40.9, 40.3, 30.7, 29.9, 25.3, 16.5 ppm; MS-ESI$^+$: *m*/*z* 646, $[M+H]^+$; HRMS-ESI$^+$: $[M+H]^+$ calcd for $C_{36}H_{44}N_3O_6S$: 646.2951, found 646.2957. Anal. Calcd for $C_{36}H_{43}N_3O_6S{\cdot}2/5\ CHCl_3$: C, 63.04; H, 6.31; N, 6.06; N, 5.90. Found: C, 63.31; H, 5.94; N, 5.65 (retrieved from the NMR sample).

4.1.5.9. (*A*)-(4*R*)-3-(2-Benzyl-3-(2-(2,6-dimethylphenoxy)acetamido)-2-hydroxypropanoyl)-*N*-((1*S*,2*R*)-2-hydroxy-1-indanyl)-5,5-dimethylthiazolidine-4-carboxamide ((*S*)-18). Compound (*S*)-**18** was synthesized according to the general procedure from (*S*)-**12** (36.2 mg, 0.080 mmol), **21** (17.5 mg, 0.097 mmol), PyBOP (63.0 mg, 0.12 mmol) and DIEA (30.0 μl, 0.18 mmol). It was purified (RP-HPLC) to give (*S*)-**18** as a white solid (26.3 mg, 52%). Compound (*S*)-**18**: t_R = 17.94 min (SP-HPLC, 15% *i*PrOH in *i*Hex); $[\alpha]_D^{21}$ = +12.1 (*c* 0.942, MeOH); ^{1}H NMR (400 MHz, CD_3OD): δ = 7.31–7.14 (m, 9H), 7.03 (d, *J* = 7.4 Hz, 2H), 6.95 (dd, *J* = 8.3, 6.5 Hz, 1H), 5.19 (dd, *J* = 4.8, 0.6 Hz, 1H), 4.92 (d, *J* = 10.8 Hz, 1H), 4.47 (ddd, *J* = 4.9, 4.8, 1.6 Hz, 1H), 4.39 (s, 1H), 4.34 (d, *J* = 14.8 Hz, 1H), 4.250 (d, *J* = 10.8 Hz, 1H), 4.245 (d, *J* = 14.8 Hz,

1H), 3.73 (s, 2H), 3.16 (d, *J* = 13.5 Hz, 1H), 2.95 (d, *J* = 13.5 Hz, 1H), 2.85 (dd, *J* = 16.5, 4.9 Hz, 1H), 2.76 (dd, *J* = 16.4, 1.6 Hz, 1H), 2.31 (s, 6H), 1.46 (s, 3H), 1.42 ppm (*s*, 3H); ^{13}C NMR (100 MHz, CD_3OD): δ = 174.6, 172.1, 171.6, 156.1, 142.0, 141.7, 137.1, 131.9, 131.5, 130.1, 129.5, 129.0, 128.1, 127.7, 126.2, 125.8, 125.2, 81.4, 75.9, 73.9, 71.3, 59.4, 50.6, 50.3, 48.9, 44.3, 40.1, 28.9, 25.6, 16.5 ppm; MS-ESI$^+$: *m*/*z* 632, [*M*+H]$^+$; HRMS-ESI$^-$: [*M*–H]$^+$ calcd for $C_{35}H_{40}N_3O_6S$: 630.2638, found 630.2636.

4.1.5.10. (*B*)-(4*R*)-3-(2-Benzyl-3-(2-(2,6-dimethylphenoxy)acetamido)-2-hydroxypropanoyl)-*N*-((1*S*,2*R*)-2-hydroxy-1-indanyl)-5,5-dimethylthiazolidine-4-carboxamide ((*R*)-18). Compound (*R*)-**18** was synthesized according to the general procedure from (*R*)-**12** (16.3 mg, 0.036 mmol), **21** (7.8 mg, 0.043 mmol), PyBOP (28.1 mg, 0.054 mmol) and DIEA (20.0 μl, 0.12 mmol). It was purified (RP-HPLC) to give (*R*)-**18** as a white solid (12.9 mg, 57%). Compound (*R*)-**18**: t_R = 13.95 min (SP-HPLC, 15% *i*PrOH in *i*Hex); $[\alpha]_D^{22}$ = +11.1 (*c* 0.83, MeOH); rotamer ratio (3:2), ^{1}H NMR (400 MHz, CD_3OD): major conformer: δ = 7.33–7.11 (m, 9H), 7.05–6.99 (m, 2H), 6.95 (m, 1H), 5.33 (d, *J* = 5.0 Hz, 1H), 5.29 (d, *J* = 10.5 Hz, 1H), 4.66 (d, *J* = 10.5 Hz, 1H), 4.60 (dt, *J* = 5.0, 1.4 Hz, 1H), 4.44 (s, 1H), 4.25 (s, 2H), 3.77 (d, *J* = 13.6 Hz, 1H), 3.55 (d, *J* = 13.6 Hz, 1H), 3.16 (d, *J* = 13.8 Hz, 1H), 3.11 (dd, *J* = 16.5, 5.0 Hz, 1H), 3.05 (d, *J* = 13.8 Hz, 1H), 2.90 (dd, *J* = 16.5, 1.4 Hz, 1H), 2.26 (s, 6H), 1.57 (s, 3H), 1.51 ppm (s, 3H); minor conformer: δ = 7.33–7.11 (m, 9H), 7.05–6.99 (m, 2H), 6.95 (m, 1H), 5.22 (d, *J* = 5.2 Hz, 1H), 4.76 (d, *J* = 10.7 Hz, 1H), 4.69 (s, 1H), 4.57 (dt, *J* = 5.2, 2.4 Hz, 1H), 4.56 (d, *J* = 10.7 Hz, 1H), 4.30 (d, *J* = 14.9 Hz, 1H), 4.17 (d, *J* = 14.9 Hz, 1H), 3.89 (d, *J* = 13.5 Hz, 1H), 3.58 (d, *J* = 13.5 Hz, 1H), 3.20 (d, *J* = 13.2 Hz, 1H), 3.02 (dd, *J* = 16.3, 5.2 Hz, 1H), 2.88 (d, *J* = 13.2 Hz, 1H), 2.86 (dd, *J* = 16.3, 2.4 Hz, 1H), 2.27 (s, 6H), 1.34 (s, 3H), 0.81 ppm (s, 3H); ^{13}C NMR (100 MHz, CD_3OD): major conformer: δ = 174.3, 173.2, 172.0, 156.0, 142.0, 141.81, 136.5, 132.0, 131.7, 130.13, 129.3, 129.0, 127.9, 127.8, 126.18, 125.8, 125.4, 80.6, 76.1, 73.9, 71.3, 59.3, 50.7, 50.5, 47.5, 43.9, 40.4, 30.0, 25.1, 16.6 ppm; minor conformer: δ = 174.8, 172.9, 171.9, 156.1, 142.3, 141.84, 137.3, 131.9, 131.7, 130.07, 129.4, 129.1, 128.0, 127.8, 126.19, 125.7, 125.4, 82.9, 76.1, 73.2, 71.2, 58.8, 51.9, 50.1, 45.7, 43.9, 40.6, 31.0, 25.4, 16.5 ppm; MS-ESI$^+$: *m*/*z* 632, [*M*+H]$^+$; HRMS-ESI$^-$: [*M*–H]$^+$ calcd for $C_{35}H_{40}N_3O_6S$: 630.2638, found 630.2653.

4.1.5.11. (*A*)-(5*R*)-*N*-((1*S*,2*R*)-2-Hydroxy-1-indanyl)-1-(2-(2,6-dimethylphenoxyacetyl)amino-2-hydroxy-4-phenylbutanoyl)pyrrolidine-5-carboxamide ((*A*)-19). Compound (*A*)-**19** was synthesized according to the general procedure from (*A*)-**13** (27.5 mg, 0.065 mmol), **21** (13.7 mg, 0.076 mmol), PyBOP (39.5 mg, 0.076 mmol) and DIEA (21.7 μl, 0.13 mmol). It was purified (RP-HPLC) to give (*A*)-**19** as a white solid (17.8 mg, 45%). (*A*)-**19**: Rotamer ratio (8:1); ^{1}H NMR (400 MHz, CD_3OD): δ = 7.38–6.85 (m, 12H), 5.24 (d, *J* = 5.0 Hz, 1H), 4.55 (dd, *J* = 8.1, 5.6 Hz, 1H), 4.48 (dt, *J* = 5.0, 1.7 Hz, 1H), 4.29 (d, 14.8 Hz, 1H), 4.25 (d, *J* = 14.8 Hz, 1H), 4.13–4.06 (m, 1H), 4.05–3.97 (m, 1H), 3.85 (d, *J* = 13.5 Hz, 1H), 3.69 (d, *J* = 13.5 Hz, 1H), 3.03 (dd, *J* = 16.4, 5 Hz, 1H), 2.85 (dd, *J* = 16.4, 1.7 Hz, 1H), 2.82–2.67 (m, 2H), 2.24–2.13 (m, 3H), 2.21 (s, 6H), 2.02–1.87 ppm (m, 3H); ^{13}C NMR (100 MHz, CD_3OD): δ = 175.2, 174.7, 171.8, 156.0, 143.3, 142.1, 141.5, 131.8, 130.0, 129.5, 129.4, 128.8, 127.6, 126.9, 125.9, 125.7, 125.7, 79.3, 74.1, 71.2, 63.8, 58.9, 50.2, 46.9, 40.7, 39.3, 30.7, 29.9, 26.9, 16.5 ppm; MS-ESI$^+$: *m*/*z* 600, [*M*+H]$^+$; HRMS-ESI$^+$: [*M*+H]$^+$ calcd for $C_{35}H_{42}N_3O_6$: 600.3074, found 600.3071. Anal. Calcd for $C_{35}H_{41}N_3O_6 \cdot 1 \cdot 1/4$ HCOOH: C, 66.24; H, 6.67; N, 6.39. Found: C, 65.96; H, 6.83; N, 6.11.

4.1.5.12. (*B*)-(5*R*)-*N*-((1*S*,2*R*)-2-Hydroxy-1-indanyl)-1-(2-(2,6-dimethylphenoxyacetyl)amino-2-hydroxy-4-phenylbutanoyl)pyrrolidine-5-carboxamide ((*B*)-19). Compound (*B*)-**19** was synthesized according to the general procedure from (*B*)-**13** (26.0 mg, 0.062 mmol), **21** (13.6 mg, 0.076 mmol), PyBOP (39.4 mg, 0.076 mmol) and DIEA (21.6 μl, 0.13 mmol). It was purified (RP-HPLC) to give (*B*)-**19** as a white solid (1.64 mg, 4.3%). Compound (*B*)-**19**: Rotamer ratio (5:1) ^{1}H NMR (400 MHz, CD_3OD): δ = 7.37–6.87 (m, 12H), 5.24 (d, *J* = 4.8 Hz, 1H), 4.49 (dt, *J* = 4.9, 1.5 Hz, 1H), 4.31 (d, 16.3 Hz, 1H), 4.29 (s, 1H), 4.22 (d, *J* = 16.3 Hz, 1H), 4.14–3.98 (m, 2H), 3.81 (d, *J* = 13.8 Hz, 1H), 3.69 (d, *J* = 13.8 Hz, 1H), 3.06 (dd, *J* = 16.5, 4.9 Hz, 1H), 2.85 (d, *J* = 16.5 Hz, 1H), 2.82–2.78 (m, 1H), 2.75–2.66 (m, 1H), 2.37–2.30 (m, 1H), 2.22 (s, 6H), 2.18–2.11 (m, 2H), 2.02–1.91 ppm (m, 3H); ^{13}C NMR (100 MHz, CD_3OD): δ = 175.3, 174.7, 171.8, 156.0, 143.3, 141.5, 131.8, 130.04, 130.01, 129.46, 129.45, 128.8, 127.8, 126.9, 125.9, 125.9, 125.7, 79.3, 74.1, 71.2, 63.8, 58.9, 50.3, 46.9, 40.7, 39.3, 30.8, 29.9, 26.9, 16.5 ppm; MS-ESI$^+$: *m*/*z* 600, [*M*+H]$^+$; HRMS-ESI$^+$: [*M*+H]$^+$ calcd for $C_{35}H_{42}N_3O_6$: 600.3074, found 600.3069.

4.1.5.13. (*A*)-(2*S*)-*N*-((1*S*,2*R*)-2-Hydroxy-1-indanyl)-2-((2-phenethyl-3-(2-(2,6-dimethylphenoxy)acetamido)-2-hydroxypropanoyl)amino)-3-phenyl-propylamide ((*A*)-20). Compound (*A*)-**20** was synthesized according to the general procedure for the epoxide opening using (*A*)-**14** (22.6 mg, 0.48 mmol) and then proceeding with **21** (10.4 mg, 0.058 mmol), HOBT (9.7 mg, 0.072 mmol) and EDC (13.8 mg, 0.072 mmol) that was dissolved in freshly distilled CH_2Cl_2 and stirred at room temperature for 30 h. It was isolated (silica, EtOAc/MeOH, 98:2–92.5:7.5) and further purified by RP-HPLC to give (*A*)-**20** (16.4 mg, 53%) as a white solid. Compound (*A*)-**20**: t_R = 21.82 min (SP-HPLC, 15% *i*PrOH in *i*Hex); $[\alpha]_D^{21}$ = −3.8 (*c* 0.153, MeOH); ^{1}H NMR (400 MHz, CD_3OD): δ = 7.35–7.32 (m, 2H), 7.26–7.06 (m, 10H) , 7.03–6.88 (m, 5H), 5.29 (d, *J* = 5.1 Hz, 1H), 4.87 (dd, *J* = 10.1, 4.7 Hz, 1H), 4.51 (ddd, *J* = 5.2, 5.1, 2.0 Hz, 1H), 4.23 (d, *J* = 14.9 Hz, 1H), 4.14 (d, *J* = 14.9 Hz, 1H), 3.68 (d, *J* = 13.7 Hz, 1H), 3.48 (d, *J* = 13.7 Hz, 1H), 3.32 (dd, *J* = 14.0, 4.7 Hz, 1H), 3.11 (dd, *J* = 16.3, 5.1 Hz, 1H), 3.01 (dd, *J* = 14.0, 10.1 Hz, 1H), 2.91 (dd, *J* = 16.3, 2.0 Hz, 1H), 2.48–2.35 (m, 1H), 2.19 (s, 6H), 2.00–1.85 (m, 2H), 1.72–1.63 ppm (m, 1H); ^{13}C NMR (100 MHz, CD_3OD): δ = 176.3, 173.7, 172.2, 156.0, 143.2, 142.0, 141.7, 138.4, 131.8, 130.5, 130.1, 129.6, 129.4, 129.3, 129.0, 128.0, 127.8, 126.8, 126.1, 125.7, 125.4, 78.4, 74.0, 71.2, 58.8, 55.8, 47.8, 40.8, 40.1, 39.1, 30.3, 16.5 ppm; MS-ESI$^+$: *m*/*z* 650, [*M*+H]$^+$; HRMS-ESI$^+$: [*M*+H]$^+$ calcd for $C_{39}H_{42}N_3O_6$: 650.3074, found 650.3076. Anal. Calcd for $C_{39}H_{43}N_3O_6 \cdot 1/4\ H_2O$: C, 71.59; H, 6.70; N, 6.42. Found: C, 71.60; H, 6.84; N, 6.37.

4.1.5.14. (*B*)-(2*S*)-*N*-((1*S*,2*R*)-2-Hydroxy-1-indanyl)-2-((2-phenethyl-3-(2-(2,6-dimethylphenoxy)acetamido)-2-hydroxypropanoyl)amino)-3-phenyl-propylamide ((*B*)-20). Compound (*B*)-**20** was synthesized according to the general procedure for the epoxide opening using (*B*)-**14** (20.9 mg, 0.48 mmol) and then proceeding with **21** (9.3 mg, 0.051 mmol), HOBT (8.7 mg, 0.064 mmol) and EDC (12.3 mg, 0.064 mmol) that was dissolved in freshly distilled CH_2Cl_2 and stirred at room temperature for 30 h. It was isolated (silica, EtOAc/MeOH, 98:2–85.5:15) and further purified by RP-HPLC to give (*B*)-**20** (13.57 mg, 49%) as a white solid. Compound (*B*)-**20**: t_R = 15.35 min (SP-HPLC, 15% *i*PrOH in *i*Hex); $[\alpha]_D^{21}$ = −0.3 (*c* 0.321, MeOH:CH_2Cl_2 (1:1)); ^{1}H NMR (400 MHz, CD_3OD:$CDCl_3$): δ = 7.35–7.09 (m, 13H), 7.03–6.98 (m, 3H) , 6.95–6.91 (m, 1H), 5.25 (d, *J* = 5.1 Hz, 1H), 4.80 (dd, *J* = 8.5, 6.1 Hz, 1H), 4.44 (ddd, *J* = 5.1, 5.0, 2.0 Hz, 1H), 4.21 (s, 2H), 3.68 (d, *J* = 13.7 Hz, 1H), 3.35–3.31 (m, 1H) (confirmed by HSQC experiment), 3.23 (dd, *J* = 13.8, 6.1 Hz, 1H), 3.10 (dd, *J* = 13.8, 8.5 Hz, 1H), 3.06 (dd, *J* = 16.4, 5.1 Hz, 1H), 2.87 (dd, *J* = 16.4, 2.0 Hz, 1H), 2.75 (dt, *J* = 13.1, 4.6 Hz, 1H), 2.47 (dt, *J* = 13.1, 4.7 Hz, 1H), 2.22 (s, 6H), 2.10 (ddd, *J* = 13.6, 12.8, 4.7 Hz, 1H), 1.84 ppm (ddd, *J* = 13.7, 12.8, 4.6 Hz, 1H); ^{13}C NMR (400 MHz, CD_3OD:$CDCl_3$): δ = 176.0, 173.2, 171.9, 155.6, 142.9, 141.7, 141.3, 137.9, 131.4, 130.3, 130.0, 129.4, 129.22, 129.18, 128.8, 127.8, 127.7, 126.7, 125.9, 125.7, 125.2, 78.2, 73.6, 71.0, 58.5, 55.5, 47.6, 40.5, 40.0, 39.2, 30.4, 16.5 ppm; MS-ESI$^+$: *m*/*z* 650,

$[M+H]^+$; HRMS-ESI$^+$: $[M+H]^+$ calcd for $C_{39}H_{42}N_3O_6$: 650.3074, found 650.3071. Anal. Calcd for $C_{39}H_{43}N_3O_6 \cdot 1/4H_2O$: C, 71.59; H, 6.70; N, 6.42. Found: C, 71.64; H, 6.82; N, 6.42.

4.2. Enzyme assays and K_i determinations

4.2.1. Plasmepsin inhibition assays

4.2.1.1. Enzyme purification. All enzymes are expressed as inactive proenzymes using the pET expression system. Each gene was cloned into pET3a and transformed into BL21 DE3 pLysS E. coli expression cells. In brief, the enzymes were expressed as inclusion bodies as described by Westling et al.[37] The proenzyme form was recovered by dissolving the inclusion bodies in 8 M urea and refolding was done by dialysis, all using conditions identical to those described by Westling et al. Enzymes were purified to homogeneity by ion exchange chromatography.

4.2.1.2. Dissociation constant determination. The dissociation constants (K_i) for the inhibitor–enzyme complexes were determined by monitoring the decrease in chromogenic substrate hydrolysis due to the presence of inhibitors. All enzymes are expressed as proenzymes. The enzymes are self-activated and converted to the mature, catalytically active form by incubating in a 0.1 M sodium acetate pH 4.5 buffer at 37 °C for 5 min prior to starting the assay. Substrate hydrolysis was measured using a Varian Cary50 spectrophotometer with an 18 cell sample handling system. To determine the K_i value, a Michaelis–Menten curve was generated using no less than five different substrate concentrations. Two additional curves were generated with two different concentrations of inhibitors. All three curves, obtained at different concentrations of an inhibitor, were fitted simultaneously using Sigmaplot10 (Systat Software Inc) to provide the value of K_i. Eq. 1 or 2 for non-tight binding and tight binding inhibitors, respectively, gave the K_i value for the inhibitor.

$$v = \left(\frac{V_{max}}{(1+\frac{K_m}{S})(1+\frac{1}{K_i})}\right) \quad (1)$$

$$v = \frac{v_o}{2E}\left(E - I - K + \sqrt{2(E - I - K_{ap} + 4EK_{ap})}\right) \quad (2)$$

4.2.2. hCatD inhibition assay

Human liver CatD was purchased from Sigma–Aldrich, Sweden. The activities of hCatD were measured essentially as described earlier,[38] using a total reaction volume of 100 μL. hCatD was activated by incubation in the assay reaction buffer (100 mM sodium acetate buffer (pH 4.5), 10% glycerol, and 0.01% Tween 20) at 37 °C for 20 min. The reaction was initiated by the addition of 3 μM substrate (DABCYL-Glu-Arg-Nle-Phe-Leu-Ser-Phe-Pro-EDANS, AnaSpec Inc, San Jose, CA, USA) and hydrolysis was recorded as the increase in fluorescence intensity over a 10-min time period, during which the rate increased linearly with time. Stock solutions of inhibitors in DMSO were serially diluted in DMSO and added directly before addition of the substrate, giving a final DMSO concentration of 1%. IC_{50} values were obtained by assuming competitive inhibition and fitting the Langmuir isotherm ($v_i/v_o = 1/(1 + [I]/IC_{50})$) to the dose–response data (Grafit), where v_i and v_o are the initial velocities of the inhibited and uninhibited reactions, respectively, and $[I]$ is the inhibitor concentration.[39] K_i values were subsequently calculated using $K_i = IC_{50}/(1 + [S]/K_m)$[40] and K_m values were determined according to Michaelis–Menten.

4.2.3. HIV-1 protease inhibition assay

The HIV-1 protease was cloned and heterologously expressed in *E. coli* and purified as described elsewhere.[41] The K_i values for the synthesized compounds were determined from two individual measurements by a fluorometric assay.[42] Assay variability was checked by inclusion of a known inhibitor and the standard deviation for the enzyme assays was ±50% of the mean.

4.2.4. In vitro anti-HIV activity assay

The in vitro anti-HIV activity was assayed in MT4 cells according to a previously published procedure.[42]

4.2.5. BACE-1 inhibition assay

BACE-1 enzyme was prepared and the inhibition of BACE-1 was determined as previously described using the Swedish mutant sequence Eu-EVNLDAEFK-Quencher as substrate.[43] IC_{50} values were determined using the following relationship: % inhibition = $100[I]/([I] + IC_{50})$.

4.3. Computational evaluation

4.3.1. Automated docking

Automated docking exploration was performed with GOLD version 3.0.1,[44] allowing full flexibility for the ligand while keeping the protein fixed (i.e., only rotation of the protein hydroxyl groups was considered). Each docking exploration consisted of 10 independent runs, using the default genetic algorithm (GA) search parameters and the Goldscore function for scoring. Parallel docking runs were performed considering either Asp214 or Asp34 in the protonated (neutral) state, while maintaining the other Asp negatively charged. A hydrogen bond distance restraint was imposed to guide docking between one of the catalytic aspartates and the hydroxyl TS mimic of the inhibitor. The protein model used was PmPM4, in the conformation adopted upon binding of **KNI-764** (PDB entry 2ANL).[13] Docking solutions were selected for post-processing only if they satisfied the following conditions: (1) The existence of a minimum hydrogen bond network between protein and ligands (minimum 3H bonds), and (2) complementarity of the four inhibitor sidechains (P2 to P2′) in the four protein binding pockets (S2 to S2). The poses selected this way were translated into PfPM4 for the next modelling step by superimposing the resulting inhibitor–2ANL complex onto the crystal structure of PfPM4 (PDB entry 1LS5). Manual docking was alternatively performed by building the inhibitor with Maestro, followed by energy minimization in Macromodel version 9.5 M (Schrödinger, New York, 2007) (1000 iteration steepest descendent steps, with H-bond restraints with the protein) in the extended conformation. Two manual conformations were considered: the first used as scaffold **KNI-764** in PmPM4 (PDB code 2ANL). The second one was a flipped conformation, in which P1 and P2 substituents were interchanged with the P1′ and P2′, respectively.

4.3.2. Molecular dynamics and binding free energy calculations

Molecular dynamics (MD) simulations were done using the program Q[45] and the OPLS force field there implemented.[46] The system was solvated with a simulation sphere of TIP3P waters[47] of radius 20 Å, centred on the α-carbon of the transition-state mimicking P1. The water surface of this sphere was subjected to radial and polarization restraints in order to mimic bulk water at the sphere boundary.[45] Non-bonded interaction energies were calculated up to a 10 Å cut-off, except for the ligand atoms for which no cut-off was used. Beyond the cut-off, long-range electrostatics were treated with the local reaction field (LRF) multipole expansion method.[48] Protein atoms outside the simulation sphere were restrained to their initial positions, and only interacted with the system through bonds, angles and torsions. For the ligand−protein simulations, a heating and equilibration procedure was applied before the data collection phase. The equilibration protocol started with 1000 steps MD using very short time step (0.2 fs) at 1 K tem-

perature, coupled to a strong bath (0.2 fs bath coupling) with positional restraints on heavy atoms. Then the system was gradually heated up to 300 K, relaxing the bath coupling to 100 fs and increasing the timestep to 1.5 fs. During this equilibration process positional restraints on the protein heavy atoms and the central atom of the ligand were gradually released from 200 to 0 kcal/(mol Å^2). The production phase followed for 1.5–1.8 ns and collecting energies at regular intervals of 15 fs. Stability was addressed by comparing the average potential energy values of the first and second halves of the data collection period. Error estimates in the calculated free energies were obtained from the appropriate scaling of these errors from the water and protein simulations, through the use of the linear interaction energy (LIE) α and β factors. The MD sampling of the free ligand was again done in a TIP3P water sphere of the same radius as in the corresponding protein simulation. The sphere was equilibrated with a 10.2 ps MD run at 300 K, with positional restraints on the heavy atoms of the ligand (200 kcal/(mol Å^2) for the first 0.2 ps and 10 kcal/(mol Å^2) in the following 10 ps). MD followed for more than 1.5 ns under the same conditions as for the bound state, but keeping the initial position of the central atom of the ligand fixed with 10 kcal/(mol Å^2) to ensure homogeneous solvation. Binding affinities were calculated using the linear interaction energy (LIE) method, described in detail elsewhere.[49,50] Basically, this approach estimates the ligand free energy of binding from the difference in the ligand−surrounding interaction energies in both its bound and free state. The relationship between the ligand intermolecular interaction energies and the free energy of binding is given by Eq. 3:

$$\Delta G_{\text{bind}} = \alpha\Delta\langle V_{l-s}^{vdw}\rangle + \beta\Delta\langle V_{l-s}^{el}\rangle + Y \quad (3)$$

where $\langle V_{l-s}^{vdw}\rangle$ and $\langle V_{l-s}^{el}\rangle$ denote, respectively, the Lennard–Jones and electrostatic interactions between the ligand and its surroundings (l–s). These interactions are evaluated as energy averages (denoted by the open brackets) from the two separate MD simulations of the free (solvated in water) and bound states. The difference (Δ) between such averages for each type of potential is scaled by different coefficients,[50] giving the polar and non-polar contributions to the binding free energy. For the non-polar contribution, this coefficient has been empirically set to $\alpha = 0.181$, while for the polar contribution the scaling factor is dependent on the chemical nature of the ligand. For ligands considered in this work the value is $\beta = 0.33$.

Acknowledgements

The authors from Uppsala University would like to acknowledge the Swedish Foundation for Strategic Research, the Swedish Research Council and Alice and Knut Wallenberg's Foundation for financial support, Professor Anders Hallberg for valuable intellectual contributions, Mr. Jonas Sävmarker and Dr. Luke Odell for purification of intermediates, Dr. Aleh Yahorau for performing the HRMS experiments and Medivir AB, Huddinge, Sweden, for conducting the inhibition assays with hCatD, HIV-1 protease and BACE-1. HGT is an Isidro Parga Pondal Research fellow (Xunta de Galicia, Spain) and acknowledges a bursary from mobility research program of Xunta de Galicia, for the stay at Uppsala University. Supercomputational centre of Galicia—CESGA has provided the computer allocation time.

Supplementary data

Supplementary data associated with this article can be found, in the online version, at doi:10.1016/j.bmc.2009.06.065.

References and notes

1. *World Malaria Report 2008*, Geneva: World Health Organisation, 2008, 1.
2. White, N. J. J. *Clin. Invest.* **2004**, *113*, 1084.
3. Goldberg, D. E.; Slater, A. F.; Cerami, A.; Henderson, G. B. *Proc. Natl. Acad. Sci. U.S.A.* **1990**, *87*, 2931.
4. Coombs, G. H.; Goldberg, D. E.; Klemba, M.; Berry, C.; Kay, J.; Mottram, J. C. *Trends Parasitol.* **2001**, *17*, 532.
5. *Global burden of disease: 2004 update* Geneva: World Health Organization, 2004.
6. Dame, J. B.; Reddy, G. R.; Yowell, C. A.; Dunn, B. M.; Kay, J.; Berry, C. *Mol. Biochem. Parasitol.* **1994**, *64*, 177.
7. Banerjee, R.; Liu, J.; Beatty, W.; Pelosof, L.; Klemba, M.; Goldberg, D. E. *Proc. Natl. Acad. Sci. U.S.A.* **2002**, *99*, 990.
8. Ersmark, K.; Samuelsson, B.; Hallberg, A. *Med. Res. Rev.* **2006**, *26*, 626.
9. Luksch, T.; Chan, N. S.; Brass, S.; Sotriffer, C. A.; Klebe, G.; Diederich, W. E. *Chemmedchem.* **2008**, *3*, 1323.
10. Hidaka, K.; Kimura, T.; Ruben, A. J.; Uemura, T.; Kamiya, M.; Kiso, A.; Okamoto, T.; Tsuchiya, Y.; Hayashi, Y.; Freire, E.; Kiso, Y. *Bioorg. Med. Chem.* **2008**, *16*, 10049.
11. Dame, J. B.; Yowell, C. A.; Omara-Opyene, L.; Carlton, J. M.; Cooper, R. A.; Li, T. *Mol. Biochem. Parasitol.* **2003**, *130*, 1.
12. Li, T.; Yowell, C. A.; Beyer, B. B.; Hung, S.-H.; Westling, J.; Lam, M. T.; Dunn, B. M.; Dame, J. B. *Mol. Biochem. Parasitol.* **2004**, *135*, 101.
13. Clemente, J. C.; Govindasamy, L.; Madabushi, A.; Fisher, S. Z.; Moose, R. E.; Yowell, C. A.; Hidaka, K.; Kimura, T.; Hayashi, Y.; Kiso, Y.; Agbandje-McKenna, M.; Dame, J. B.; Dunn, B. M.; McKenna, R. *Acta Crystallogr., Sect. D* **2006**, *62*, 246.
14. Omara-Opyene, A. L.; Moura, P. A.; Sulsona, C. R.; Bonilla, J. A.; Yowell, C. A.; Fujioka, H.; Fidock, D. A.; Dame, J. B. *J. Biol. Chem.* **2004**, *279*, 54088.
15. Liu, J.; Gluzman, I. Y.; Drew, M. E.; Goldberg, D. E. *J. Biol. Chem.* **2005**, *280*, 1432.
16. Bonilla, J. A.; Bonilla, T. D.; Yowell, C. A.; Fujioka, H.; Dame, J. B. *Mol. Microbiol.* **2007**, *65*, 64.
17. Nezami, A.; Kimura, T.; Hidaka, K.; Kiso, A.; Liu, J.; Kiso, Y.; Goldberg, D. E.; Freire, E. *Biochemistry* **2003**, *42*, 8459.
18. Kiso, A.; Hidaka, K.; Kimura, T.; Hayashi, Y.; Nezami, A.; Freire, E.; Kiso, Y. *J. Pept. Sci.* **2004**, *10*, 641.
19. Ekegren, J. K.; Unge, T.; Safa, M. Z.; Wallberg, H.; Samuelsson, B.; Hallberg, A. *J. Med. Chem.* **2005**, *48*, 8098.
20. Ekegren, J. K.; Gising, J.; Wallberg, H.; Larhed, M.; Samuelsson, B.; Hallberg, A. *Org. Biomol. Chem.* **2006**, *4*, 3040.
21. Wu, X. Y.; Öhrngren, P.; Ekegren, J. K.; Unge, J.; Unge, T.; Wallberg, H.; Samuelsson, B.; Hallberg, A.; Larhed, M. *J. Med. Chem.* **2008**, *51*, 1053.
22. Beyer, B. B.; Johnson, J. V.; Chung, A. Y.; Li, T.; Madabushi, A.; Agbandje-McKenna, M.; McKenna, R.; Dame, J. B.; Dunn, B. M. *Biochemistry* **2005**, *44*, 1768.
23. Howard-Lock, H. E.; Lock, C. J. L.; Martins, M. L.; Smalley, P. S.; Bell, R. A. *Can. J. Chem.* **1986**, *64*, 1215.
24. Yamansarova, E. T.; Kukovinets, A. G.; Kukovinets, O. S.; Zainullin, R. A.; Galin, F. Z.; Kunakova, R. V.; Zorin, V. V.; Tolstikov, G. A. *Russ. J. Org. Chem.* **2001**, *37*, 246.
25. Westling, J.; Yowell, C. A.; Majer, P.; Erickson, J. W.; Dame, J. B.; Dunn, B. M. *Exp. Parasitol.* **1997**, *87*, 185.
26. For a review, see: Bjelic, S.; Nervall, M.; Gutierrez-de-Terán, H.; Ersmark, K.; Hallberg, A.; Åqvist, J. *Cell. Mol. Life Sci.* **2007**, *64*, 2285.
27. Gutiérrez-de-Terán, H.; Nervall, M.; Ersmark, K.; Liu, P.; Janka, L. K.; Dunn, B.; Hallberg, A.; Åqvist, J. *Biochemistry* **2006**, *45*, 10529.
28. Hidaka, K.; Kimura, T.; Tsuchiya, Y.; Kamiya, M.; Ruben, A. J.; Freire, E.; Hayashi, Y.; Kiso, Y. *Bioorg. Med. Chem. Lett.* **2007**, *17*, 3048.
29. Brynda, J.; Rezacova, P.; Fabry, M.; Horejsi, M.; Stouracova, R.; Sedlacek, J.; Soucek, M.; Hradilek, M.; Lepsik, M.; Konvalinka, J. *J. Med. Chem.* **2004**, *47*, 2030.
30. Janka, L.; Clemente, J.; Vaiana, N.; Sparatore, A.; Romeo, S.; Dunn, B. M. *Protein Pept. Lett.* **2008**, *15*, 868.
31. Liu, X. W.; Hu, X. E.; Tian, X. R.; Mazur, A.; Ebetino, F. H. *J. Organomet. Chem.* **2002**, *646*, 212.
32. Fraisse-Jullien, R.; Fréjaville, C. *Bull. Soc. Chim. Fr.* **1970**, 219.
33. Eistetter, K.; Wolf, H. P. O. *J. Med. Chem.* **1982**, *25*, 109.
34. Mimoto, T.; Kato, R.; Takaku, H.; Nojima, S.; Terashima, K.; Misawa, S.; Fukazawa, T.; Ueno, T.; Sato, H.; Shintani, M.; Kiso, Y.; Hayashi, H. *J. Med. Chem.* **1999**, *42*, 1789.
35. Tanimori, S.; Naka, T.; Kirihata, M. *Synth. Commun.* **2004**, *34*, 4043.
36. Thompson, W. J.; Fitzgerald, P. M. D.; Holloway, M. K.; Emini, E. A.; Darke, P. L.; Mckeever, B. M.; Schleif, W. A.; Quintero, J. C.; Zugay, J. A.; Tucker, T. J.; Schwering, J. E.; Homnick, C. F.; Nunberg, J.; Springer, J. P.; Huff, J. R. *J. Med. Chem.* **1992**, *35*, 1685.
37. Westling, J.; Cipullo, P.; Hung, S. H.; Saft, H.; Dame, J. B.; Dunn, B. M. *Protein Sci.* **1999**, *8*, 2001.
38. Haque, T. S.; Skillman, A. G.; Lee, C. E.; Habashita, H.; Gluzman, I. Y.; Ewing, T. J. A.; Goldberg, D. E.; Kuntz, I. D.; Ellman, J. A. *J. Med. Chem.* **1999**, *42*, 1428.
39. Copeland, R. A. In *Enzymes: A Practical Introduction to Structure, Mechanism, and Data Analysis*; Copeland, R. A., Ed.; VCH: New York, NY, 1996; p 300.
40. Cheng, Y.; Prusoff, W. H. *Biochem. Pharmacol.* **1973**, *22*, 3099.
41. Danielson, U. H.; Lindgren, M. T.; Markgren, P.-O.; Nillroth, U. *Adv. Exp. Med. Biol.* **1998**, *436*, 99.
42. Nillroth, U.; Vrang, L.; Markgren, P.-O.; Hulten, J.; Hallberg, A.; Danielson, U. H. *Antimicrob. Agents Chemother.* **1997**, *41*, 2383.

43. Bäck, M.; Nyhlén, J.; Kvarnström, I.; Appelgren, S.; Borkakoti, N.; Jansson, K.; Lindberg, J.; Nyström, S.; Hallberg, A.; Rosenquist, A.; Samuelsson, B. *Bioorg. Med. Chem.* **2008**, *16*, 9471.
44. Jones, G.; Willett, P.; Glen, R. C.; Leach, A. R.; Taylor, R. *J. Mol. Biol.* **1997**, *267*, 727.
45. Marelius, J.; Kolmodin, K.; Feierberg, I.; Åqvist, J. *J. Mol. Graph. Model.* **1998**, *16*, 213.
46. Jorgensen, W. L.; Maxwell, D. S.; TiradoRives, J. *J. Am. Chem. Soc.* **1996**, *118*, 11225.
47. Jorgensen, W. L.; Chandrasekhar, J.; Madura, J. D.; Impey, R. W.; Klein, M. L. *J. Chem. Phys.* **1983**, *79*, 926.
48. Lee, F. S.; Warshel, A. *J. Chem. Phys.* **1992**, *97*, 3100.
49. Åqvist, J.; Medina, C.; Samuelsson, J. E. *Protein Eng.* **1994**, *7*, 385.
50. Hansson, T.; Marelius, J.; Åqvist, J. *J. Comput. Aided Mol. Des.* **1998**, *12*, 27.